12-2011

Air Demand in Low-Level Outlet Works

Jason Arthur Larchar
Utah State University

AIR DEMAND FOR LOW-LEVEL OUTLET WORKS

by

Jason A. Larchar

A thesis submitted in partial fulfillment
of the requirements for the degree

of

MASTER OF SCIENCE

in

Civil and Environmental Engineering

Approved:

Blake P. Tullis Major Professor	Steven L. Barfuss Committee Member
Paul J. Barr Committee Member	Mark R. McLellan Vice President for Research and Dean of the School of Graduate Studies

UTAH STATE UNIVERSITY
Logan, Utah

2011

ABSTRACT

Air Demand in Low-Level Outlet Works

by

Jason A. Larchar, Master of Science

Utah State University, 2011

Major Professor: Blake P. Tullis
Department: Civil and Environmental Engineering

Most dams have a low-level outlet that consists of a closed conduit through the dam with a slide gate or valve to regulate flow. These outlets are used mainly for irrigational purposes but also for flushing the reservoir and controlling the reservoir elevation. When discharging through the low-level outlet works, negative pressures can develop on the downstream side of the gate creating a potential for cavitation damage and vibration. To minimize these effects, air vents (vented to the atmosphere) are installed on the downstream side of the gate to limit downstream pressure to something above vapor pressure (i.e., near atmospheric pressure).

Previous air venting studies have been mostly limited to large dam outlet geometries, which typically feature a vertical gate in a flat-bottomed discharge tunnel. The large-dam air demand analysis has been based on the Froude number of the supercritical flow at the vena contract (located between the gate and the hydraulic jump) and the water flow rate. Small to medium-sized embankment dams typically utilize a

slide gate installed on the sloped upstream face for flow control, followed by a vertical elbow connected to a sloping pipe. With this outlet geometry, there is no 1-D vena contracta flow, no classical hydraulic jump, and no representative Froude number. Additionally, no head-discharge characteristic data have been found for inclined slide gates (vented or non-vented) for small to medium-sized dams. Consequently, unless a flow measurement structure is installed in the discharge channel downstream of the dam, determining the water discharge rate based on gate opening and head on the gate, and consequently the air demand is problematic. This study focuses on quantifying air demand and air vent sizing for the small to medium-sized embankment dam low-level outlet geometries by providing:

1. C_d values as a function of gate openings and air demand; to better estimate flow rates from outlet works of similar geometries.
2. Flow conditions for varying operating conditions.
3. A new relationship for sizing air vents as a function of driving head and gate opening.
4. The magnitude of negative pressures for non-vented conduits.
5. A foundation for future studies and development of air demand research.

This thesis presents the findings of this study.

(74 pages)

ACKNOWLEDGMENTS

I am in gratitude to several people who have aided in the process of this research. My thanks go to the following: Blake Tullis for provided the opportunity and employment at the Utah Water Research Laboratory (UWRL); my committee members, Steve Barfuss and Paul Barr, for continued guidance in the research process; and Amanda Laurendeau who aided in much of the data collection. In addition, I would like to thank The Utah State Office of Dam Safety for provided initial funding for this air vent research, and continued funding by the USGS (United States Geological Survey) and the Utah Water Research Laboratory (UWRL). Lastly I would like to thank my family and especially wife, Rachel, for her continued support as I have worked toward my graduate degree.

Jason A. Larchar

CONTENTS

Page

LIST OF TABLES

LIST OF FIGURES

LIST OF ACRONYMS AND ABBREVIATIONS

cfm	cubic feet per minute
cfs	cubic feet per second
cms	cubic meters per second
fpm	feet per minute
fps	feet per second
ft	feet
lb	pound force
m	meter
N	newton
s	seconds
UWRL	Utah Water Research Laboratory
USBR	United States Bureau of Reclamation

LIST OF SYMBOLS

A	Cross-sectional area of pipe, ft (m)
C_d	Valve discharge coefficient
d	Diameter of orifice throat, ft (m)
D	Diameter of pipe, ft (m)
Fr	Froude number
γ	Specific weight of water lb/ft^3, (N/m^3)
g	Acceleration due to gravity, ft/s^2 (m/s^2)
H	Total energy head, ft (m)
v	Maximum water surface velocity conduit, fps (mps)
Q_a	Air flow rate measured through air vent, cfs (cms)
Q_w	Water flow rate in conduit, cfs (cms)
Re	Reynolds number of discharge or flow rate
β	Beta, (Q_a/Q_w)

CHAPTER 1

INTRODUCTION

Since the settlement of Utah, dams have been built across the state for a variety of uses including agricultural and municipal uses, hydropower, recreation, and beauty. However, with new understanding of structures and hydrologic probabilities, many dams are being stabilized or rebuilt. Unfortunately however, there still exists lack of design criteria for air vents for the low-level outlet works for such structures.

Typically, these dams have outlet works that consist of a closed conduit through the dam with a slide gate or valve to regulate flow. These outlets serve four main purposes: (*i*) control of first impounding, (*ii*) flushing the reservoir of sedimentation, (*iii*) release and monitoring of irrigation waters, and (*iv*) draw down of the reservoir for maintenance (Speerli, 2000). When in operation, negative pressures can develop on the downstream side of these valves due to the flow separation region that develops, which can cause serious damaging effects; mainly, cavitation and vibration. As the pressure differential across the valve increases, the potential for cavitation increases, which is a serious problem related to valve operation (Tullis, 1989). To minimize or eliminate these effects, air vents (vented to the atmosphere) are installed on the downstream side of the gate to relieve the negative pressures that develop. When designed correctly, the air vent will prevent the pressure from reaching vapor pressure and maintain the pressure downstream of the gate near atmospheric pressure where a safe and steady operation is achieved.

Background

Unfortunately, there is little understanding regarding air venting and design information is limited. Consequently some dams may have inadequate air vents and proper sizing techniques have yet to be established. If an air vent is adequately sized the pressure downstream of the gate will be at atmospheric pressure, creating an inlet flow control condition. As a result, any downstream conditions including tailwater elevation should not affect the discharge rate. If the air vent is insufficient or non-existent however, aside from the risks of cavitation, the flow rate and flow conditions (i.e. full pipe or open channel flow) will be greatly influenced. For such a condition, (insufficient venting resulting in full pipe flow), the driving head becomes the difference between the reservoir and the tailwater elevations, creating a greater driving head resulting in potentially a higher discharge. Free-discharging pipe outlets can also function as an air venting source under non-full pipe flow conditions.

For many large prototype dams, scaled model studies have been conducted and analyzed in order to achieve optimal design of the air vents; however, it is difficult to correlate design criteria for large dams to smaller dams spoken of in this research due to geometric differences in their outlet works. Large dams commonly have large rectangular or horseshoe shaped conduits through the dam with a vertical control gate located inside the dam as seen in Figure 1. The dam geometries considered in this research involve a circular slide gate installed on the sloping upstream face of an embankment dam, followed by a vertical elbow where flow enters the conduit as shown

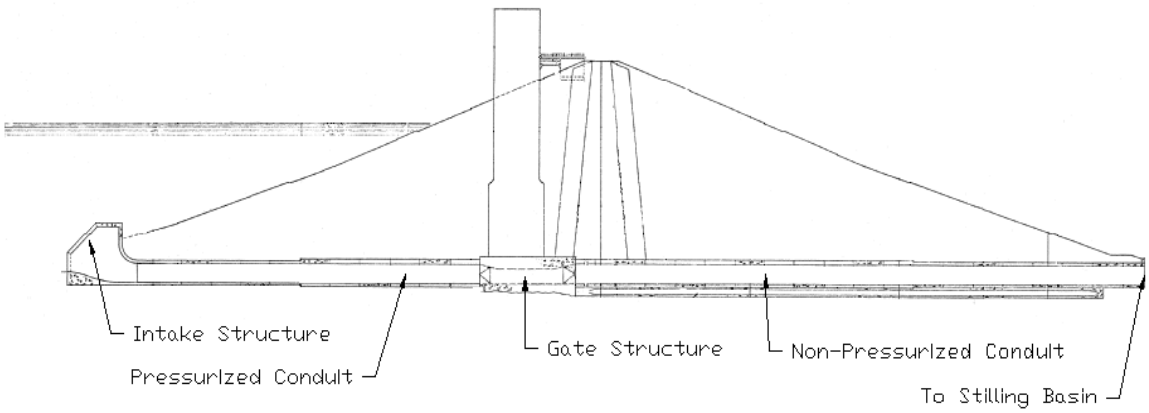

Figure 1. Large dam outlet works.

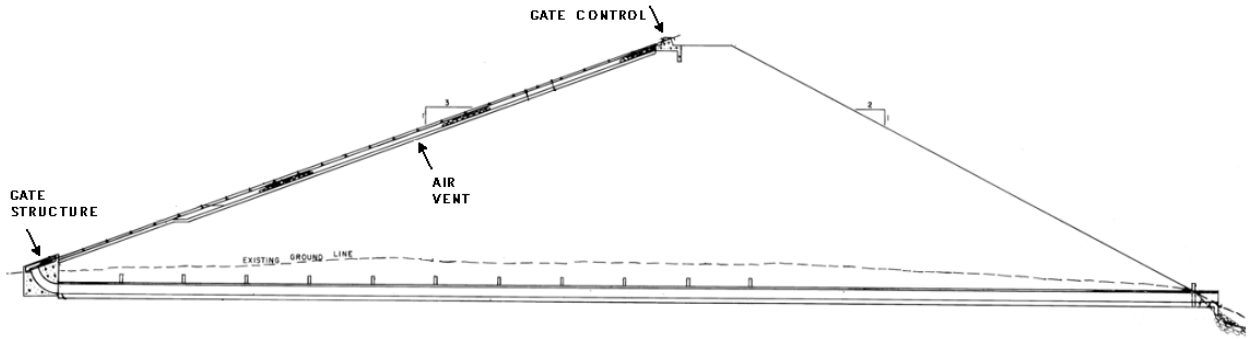

Figure 2. Small embankment dam outlet works.

in Figure 2. No studies were found in the literature addressing air demand for small- and medium-sized dam geometries consistent with Figure 2.

Objective

The purpose of this research was to establish guidelines for sizing air vents in small dams, and determine flow characteristics for various conditions. This objective was achieved by building and testing a laboratory-scale model. Since this research is in a

way a pioneering effort, it is expected that further research will be necessary to verify the findings and further explore additional scenarios. In addition, it is the intent of the author to determine discharge coefficient (C_d) values for a typical gate, and provide a description of flow conditions for typical operation of such outlet works.

Research Scope

This research was limited to examining the relationships between air demand, gate openings, and upstream head for a circular conduit outlet. Negative air pressure was measured, but for reference only. The author does not attempt to explain the causes of all the results but rather to present a basis for design for air vent sizing based on observed data. The results from this study are intended to be used for design purposes for geometrically similar outlet works and perhaps as a first order approximation of dissimilar designs in the absence of better design data. The physical experimental setup, methods, and procedures used in this study are described in detail in Chapter 4.

Overview

In an effort to understand what work has been previously done on the subject a literature review was conducted. Unfortunately very little of the published literature found, however, was directly applicable to the research topic. An overview of the literature review is found in Chapter 2. Chapter 3 contains an in-depth description of the physical setup of the experiment, procedures, and data collection process used to obtain data. Additional theory applicable to the data collection process is presented as well.

The experimental results are presented in Chapter 4, and an example of the application of this research in the design realm is outlined in Chapter 5. The conclusions of the research including a summary and recommendation for further research are presented in Chapter 6.

CHAPTER 2

LITERATURE REVIEW AND THEORY

Literature Review

Over the past century, many have attempted studies to create relationships for estimating air demand in closed conduits. It is important to note that the majority of work regarding air venting has been specific to large dam low-level outlet geometries.

One of the first studies conducted regarding air demand in closed conduits was conducted by Kalinske and Robertson (1943) who studied air demand in relation to a hydraulic jump in a circular closed conduit and determined air demand was a function of the Froude number upstream of the jump. Their results have been analyzed and slightly modified by several researchers, providing a basis for estimating air demand for such applications (USCE, 1964; Campbell and Guyton, 1953; Wisner, 1965 as cited in Sharma, 1976; Levin, 1965, as cited by Speerli, 2000). Kalinske and Robertson added that above a critical condition, the air demand was a function of the ability of the hydraulic jump to entrain air; and below this critical condition too much air is entrained in the flow and the air removal is then based on the hydraulic features of the flow (Kalinske and Robertson, 1943).

Sharma (1976) sites Dettmers (1953) as having provided some insight with his research on the Lumiei Dam, which concluded that air demand also depended on the geometry of the gate structure and was independent of head. He stated that the ratio of

air flow to water flow ($\beta = Q_a/Q_w$) was mainly influenced by the geometry of the gate structure (Sharma, 1976).

In 1966, the United States Bureau of Reclamation (USBR) performed a model study of the Silver Jack Dam Outlet Works Bypass, which features a low level outlet works for a relatively large dam. It was observed that for gate openings < 60 percent, there was negligible air flow through the air vent. For these gate openings, the aerated water did not fill the pipe and air entering the downstream end of the pipe satisfied the air demand at the gate. For gate openings between 60 percent and 80 percent, a small air flow in the vent was observed but not significant enough to be measured, however, for gate openings of 80 percent and 100 percent air demand data through the vent was recorded. It was observed that air demand was erratic in the conduit and at large gate openings was directly proportional to water discharge and changed as geometries changed (USBR, 1966).

In the aforementioned model study it was also observed that using a short downstream conduit, the air moved up the pipe even at a gate opening of 100 percent where the pipe was mostly full of aerated water. This scenario was observed with a conduit length of 3.72D (D = downstream conduit width) up to 18.5D. When the pipe was not self-venting from the downstream end, a sharp increase in air demand was observed suggesting that much of the air demand was supplied from the pipe exit. Due to the air entering the end of the pipe, it was observed that as the conduit length increased, air demand also increased (USBR, 1966). Speerli (1999) studied an experimental setup with a vertical slide gate and square tunnel varying the tunnel length from 2.3 to 20 m

and determined that the air demand is largest with a shorter outlet tunnel. Although these studies have been the basis for the design of many large dam outlet works, as shown here, their conclusions vary and much uncertainty remains in the application of their research to small dams with varying low-level outlet geometries (i.e, those without vertical slide gates and flat bottomed conduits where classical hydraulic jumps can form).

Theory Applied in This Study

Considering the relationships discussed, air demand has been identified to be a function of the Froude number (Sharma, 1976); which, for large dams is calculated using the effective depth of the vena-contracta just downstream of the gate (Falvey, 1980). This approach works relatively well for rectangular, vertical gates, but for geometries similar to that in Figure 2 featuring a sloped gate on the face of the dam and a following elbow no studies or data have been found. For a low-level small dam outlet works, the flow is similar to that of a gate valve attached to a large tank discharging into an elbow followed by a closed conduit. Thus, there is no real traditional critical flow section and there is high level of turbulence and spray. The published literature suggests differing methods for estimating air demand if flow in the conduit is either open channel or pressurized flow. Since both will be occurring, a new method of estimating air demand will be developed as a function of gate opening and driving head.

Additionally, the equations used for estimating air demand are usually displayed as a ratio called beta (β), which is equal to Q_a/Q_w. This is another potential problem since most embankment dam outlet works do not employ flow measurement devices, thus

Q_w is typically unknown. This is not only an issue in determining air demand, but also greatly complicates water resource management. Some attempts have been made to use the energy equation (Bernoulli) to determine the water flow rate but no published valve discharge coefficient or loss coefficient data have been found, making this approach impractical. If the slide gate is treated as a valve, an equation used to calculate the water flow through the valve is:

$$\Delta H = \frac{KQ^2}{2gA^2} \tag{1}$$

where:

Q	Discharge or flow rate, cfs (cms)
K	Valve loss coefficient
A	Cross-sectional area of pipe, ft^2 (m^2)
g	Acceleration due to gravity, ft/s^2 (m/s^2)
ΔH	Change in total head across the valve, ft (m) (Tullis, 1989)

The valve loss coefficient can be converted to a discharge coefficient (C_d) that can also be used to calculate flow through a valve. A discharge coefficient is the ratio of the actual to the theoretical discharge through a valve, orifice or any such structure. It is the intent of the author to conduct a study to determine C_d values for a common gate that will enable better water discharge calculations and ultimately air demand and air vent sizing. The complete steps for the C_d calculation are found in Appendix C.

CHAPTER 3

PHYSICAL EXPERIMENTAL SETUP AND DATA COLLECTION

Physical experimental setup

All testing for this study was performed at the Utah Water Research Laboratory (UWRL) at Utah State University. The experimental setup consisted of a steel tank, 6'x3'x6' (length x width x height). The tank has an acrylic floor sloped at approximately 18 degrees (~3:1 slope) from the horizontal to simulate the upstream face of an embankment dam.

Water was supplied to the model through four-inch and two-inch flexible hoses for high and low flow rates, respectively. Water entered the tank via a four-inch diffuser and then passed through a plastic screen as well as a vertically oriented baffle, as shown in Figure 3, to eliminate flow source effects. Flow rates were metered using laboratory calibrated orifice plates located in the supply lines, and controlled using a four-inch butterfly valve or a two-inch gate valve in their respective supply line. Pressure differentials across the orifice plates were measured with manometers.

The outlet works consisted of a 3-inch acrylic conduit 60 inches in length, which attached to a 3-inch diameter mitered elbow assembly connected to the acrylic bottom of the tank. The discharge pipe was set to a slope of 4.5 percent from the horizontal for all runs. Photos of the setup can be seen in Figures 4 and 5. A 1-inch flange was inserted between the elbow and the sloped floor that contained four ½-inch holes to allow air into the outlet behind the gate. A machined gate was constructed to resemble a *Waterman* –

type sliding gate that was mounted on the sloped floor covering the 3-inch discharge hole. All test results apply to this slide gate type and therefore if other gate types are considered, the results of this study may not apply.

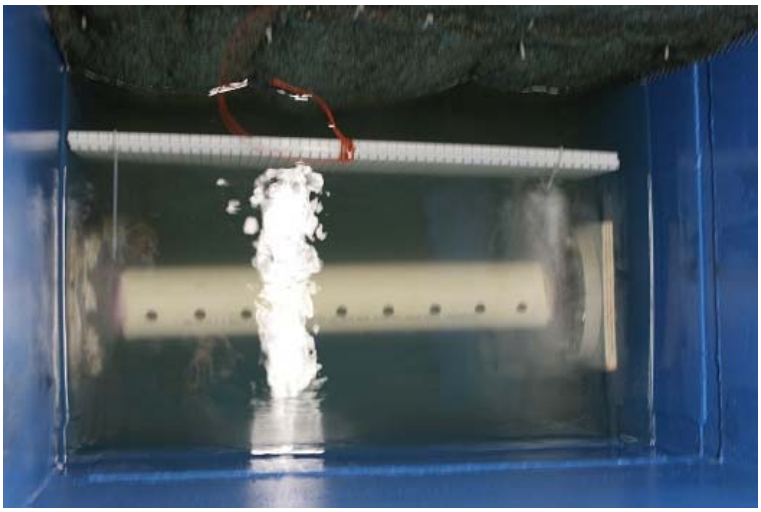

Figure 3. Flow diffuser.

Figure 4. Experimental setup.

The gate could be operated using a crank that extends to the outside of the tank to facilitate changing gate openings. Acrylic gussets were added to the floor of the tank to add stability. A picture of the sliding control gate and elbow assembly can be seen in Figure 6 and Figure 7, respectively.

Figure 5. Experimental setup including outlet.

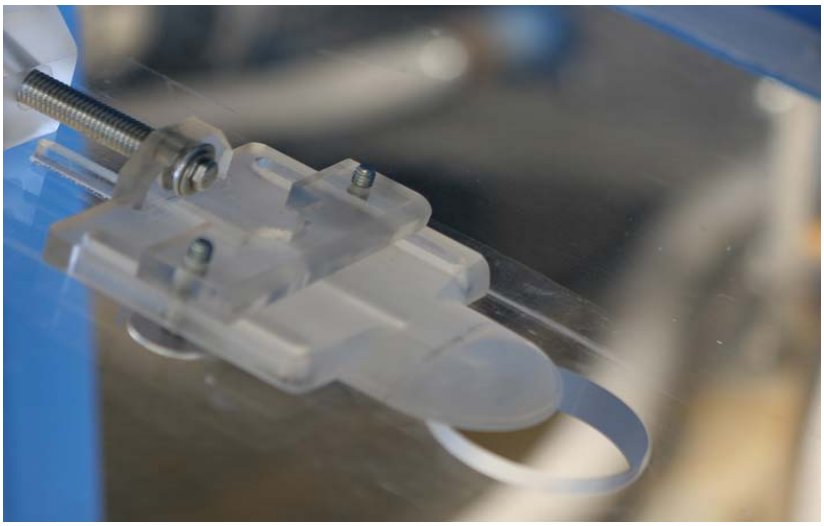

Figure 6. Slide gate (without the outlet piping installed).

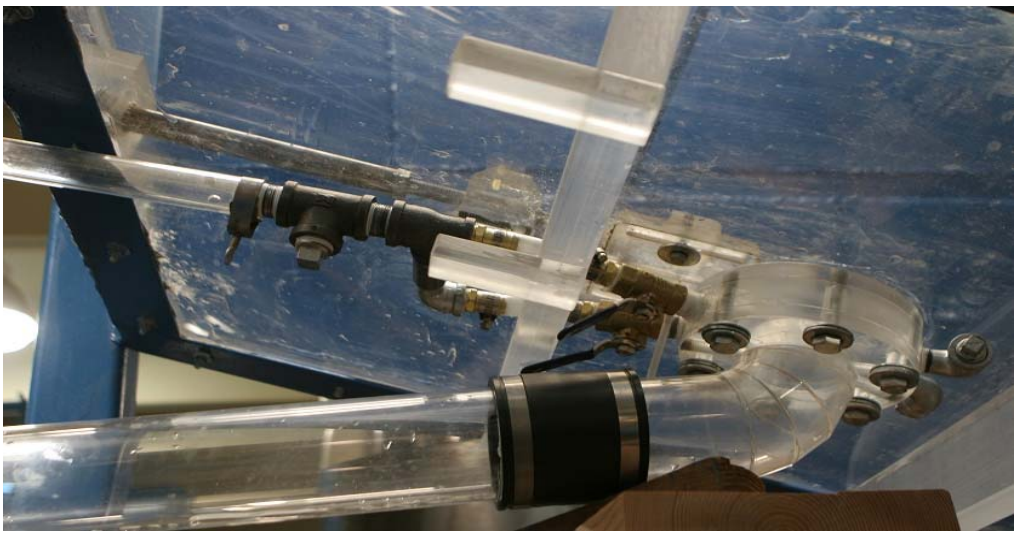

Figure 7. Elbow assembly and air vents.

Data Measurements

A series of data was collected at varying water elevations in the tank and gate openings. The first set of data included flow rates for the vented and non-vented conditions for varying water elevations and a free discharging outlet (no tailwater). For the non-vented conditions, the magnitude of negative pressures was measured using a negative pressure gauge, and for the vented conditions, air velocity was measured through the air vent using a calibrated thermal anemometer. A second set of data was collected using the same setup, however the discharge pipe was submerged preventing any air venting from the downstream end of the pipe. The two scenarios were analyzed and results are discussed in Chapter 4. Gate openings between 10 to 100 percent open were evaluated.

To ensure sufficient data for this research, several measurements were recorded including: water flow rate, piezometric head in the tank measured relative to the centerline elevation of the low-level outlet works inlet, air flow rate, and negative pressures behind the gate. Each measurement procedure is discussed below.

Water flow rate

As mentioned previously, the water flow rate was measured using calibrated orifice plates installed in the supply lines. The calibration data for the 4-in and 2-in lines can be found in Appendix A. The pressure differential was measured across the orifice plates using manometers filled with mercury (s.g. =13.56) and Meriam Blue Fluid (s.g.=1.75). The differential pressure observed with the manometers was then converted to head loss (ft) using the following conversion:

$$dh = R * 0.0328 * (\text{sg} - 1) \tag{2}$$

where:

dh	Differential across orifice plate, ft (m)
R	Difference measured on manometer, cm (in)
sg	Specific gravity of water, (dimensionless)

The value of 0.0328 is a conversion factor used to convert centimeters to inches. Two manometers were used to accommodate measuring the range of flows investigated; the mercury manometer was used only when flows exceeded the limits of the Meriam Blue fluid manometer.

After determining the head loss (ft) from the orifice plates, the water flow rate through the supply line was calculated using a macro shown in Appendix A based on the the orifice equation below:

$$Q = C_d \cdot A_o \cdot \frac{\sqrt{2 \cdot g \cdot \Delta h}}{1 - \left(d/D\right)^4} \tag{3}$$

where:

Q Discharge or flow rate, cfs (cms)

C Orifice discharge coefficient

A_O Cross-sectional area of orifice throat, ft^2 (m^2)

g Acceleration due to gravity, ft/s^2 (m/s^2)

Δh Head loss differential across orifice plate, ft (m)

d Diameter of orifice throat, ft (m)

D Diameter of pipe, ft (m)

Piezometric head in the tank

The piezometric head in the tank was measured relative to the center of the discharge hole in the floor. A pressure tap was connected to a piezometric tube mounted to the side of the tank; head measurements were made using a scale mounted to the piezometric tube. The scale was referenced to the outlet hole centerline using a survey level.

Air flow rate

Air flow velocities were measured using a Kanomax thermal anemometer (Model

A031). Two vent holes were used to supply air to the downstream side of the slide gate. These holes were plumbed together to a 1-in pipe where the anemometer was placed to measure air velocities. A picture of the air vent setup can be seen in Figure 7. Each of the two air supplies contained isolation ball valves. For vented test runs both valves were open 100 percent and for non-vented conditions, the valves were completely closed.

Initially four vents were installed, however after the first tests were run it was determined that two vents located on the inside of the elbow were adequate. With four vents operating, the two vents installed on the outside of the elbow (side opposite the air vent tubing) filled with water rather than draw air.

Negative pressure behind the gate

Negative pressures were measured for non-vented conditions through a pressure tap located behind the gate connected to a Roylyn vacuum pressure gage shown in Figure 8. Before each test session, the gage was zeroed relative to atmospheric pressure at the elevation of the pressure tap to eliminate error.

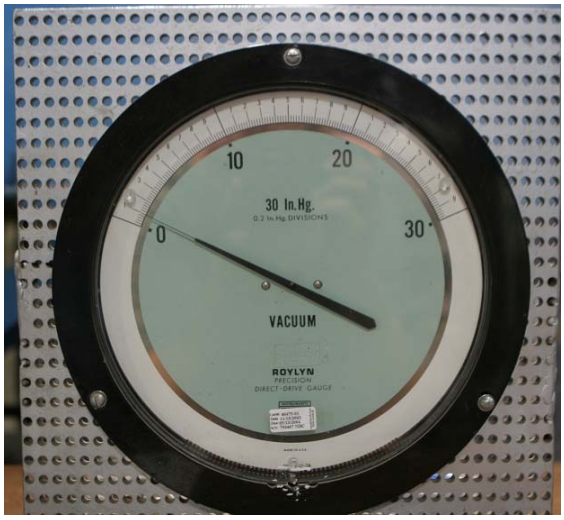

Figure 8. Vacuum pressure gage.

The gage displayed pressure in inches of mercury, which was converted to inches of water by multiplying by the specific weight of mercury. Inches of water were then converted to psi (pounds per square inch) by multiplying by the unit weight of water and dividing by 144 for dimensional continuity. There is some uncertainty in the data obtained from this procedure since all of the pressures measured were less than three inches of mercury on a scale of 0 to 30. The effects of operation at the low end of the scale are unknown.

Data Collection

Data were obtained for the following conditions:

1 Vented discharge with a non-submerged outlet

2 Non-vented discharge with a non-submerged outlet

3 Vented discharge with a submerged outlet

Submerged outlet discharge was the condition that existed when the tailwater was above the top of the discharge pipe outlet preventing aeration from the end of the pipe as shown in Figure 9. The non-submerged outlet condition (also referred to as free-discharging outlet) is also shown in Figure 9 where the flow was free flowing out the end of the pipe. Initially, data were collected for five different gate openings: 10, 30, 50, 70, and 90 percent of the linear distance of opening (see Figure 10). After some observance of the data, additional gate openings of 60 and 100 percent were explored. Percent gate opening refers to the percent of gate linear travel distance, not percentage of flow area.

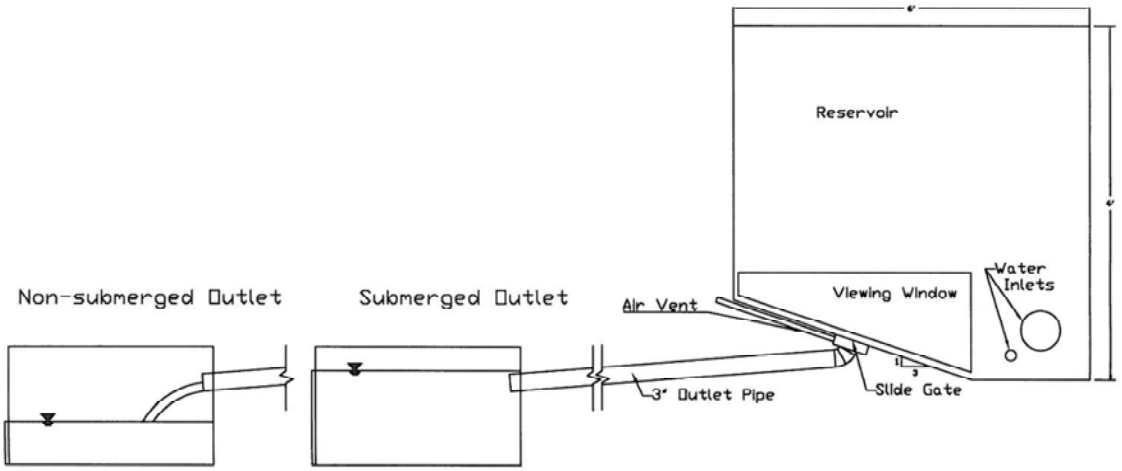

Figure 9. Tailwater conditions.

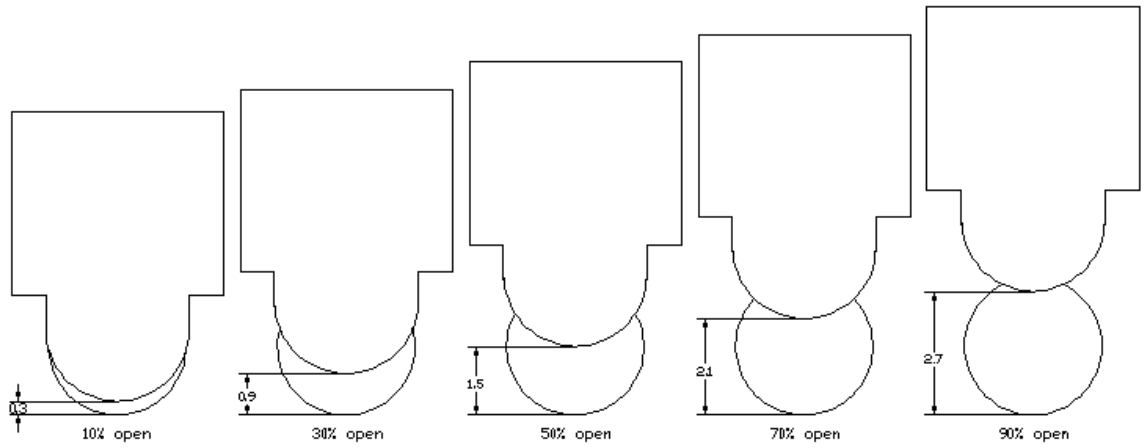

Figure 10. Slide gate positions.

For each gate opening, a series of data were obtained at varying water elevations in the tank. Target elevations included 6 inches to 66 inches at 6-inch intervals measured from the water surface elevation to the center of the discharge hole in the bottom of the tank. For each test, the flow rate was set and the water level was repeatedly monitored to achieve a constant water elevation. When needed, the flow rate was adjusted and again

the water level was allowed to stabilize. The magnitude of the negative pressure was recorded during the non-vented test only. Q_w were obtained only for the free discharging outlet condition (vented and non-vented) to develop coefficients of discharge (C_d) values for the gate positions.

During testing of the vented conditions, air velocity data were recorded for both submerged and non-submerged outlet conditions. Air velocity measurements were recorded for a minimum of 3 minutes for each run; the instrumentation obtained data at a frequency of 4 Hz.

Much effort was made to eliminate any induced vortices or organized flow patterns in the tank. To verify that no such conditions existed, red dye was injected into the flow and observed.

CHAPTER 4

EXPERIMENTAL RESULTS

Introduction

Chapter 4 includes the experimental results as well as a discussion of the findings. Many of the results are presented in graphical form and the supporting data can be found in the appropriate appendices. The major variables examined in this study that will be discussed include: Air demand based on gate opening, piezometric head in the tank, and water flow rates for submerged and non-submerged outlet conditions. C_d values are also presented for vented and non-vented conditions. The magnitude of the negative pressures will also be shown, however as mentioned, the accuracy is questionable.

Results

Air demand uncertainty

After completing several initial tests, the data showed that there was a great variation in the air flow for certain conditions for both the submerged and non-submerged outlet. Several duplicate data points were obtained to determine the repeatability of the data collected, and it was determined that the repeatability varied with different flow conditions. For low heads and smaller gate openings, the water flow was typically steady (minimal fluctuations) resulting in a steady air demand, however, the air flow for most conditions was erratic and non-repeatable.

Additional data were collected to determine if the inconsistencies were in the instrumentation limitations or phenomenological uncertainty. A control experiment was

conducted to verify the accuracy of the anemometer. Five data sets were collected with one Kanomax anemometer and three additional data sets were collected with another anemometer (identical model). Figure 11 shows that for one of the steady flow conditions, both meters yielded consistent data implying that any inconsistencies are likely not due to the air flow meter inaccuracies. Though the maximum and minimum Q_a values showed some variation, the average Q_a was very consistent. This experiment demonstrated that the instrumentation and setup was not the source of the inconsistencies. Another sample with a different gate opening yielded different results as shown in Figure 12. Although the H/d was the same, the Q_a data was not as consistent.

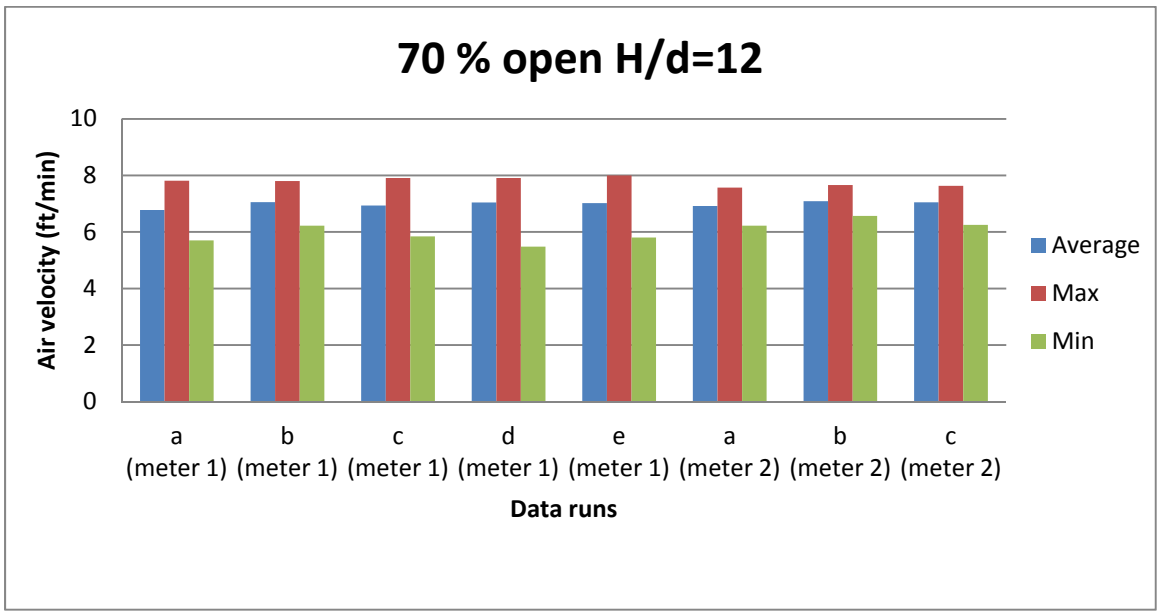

Figure 11. Accuracy experiment 1.

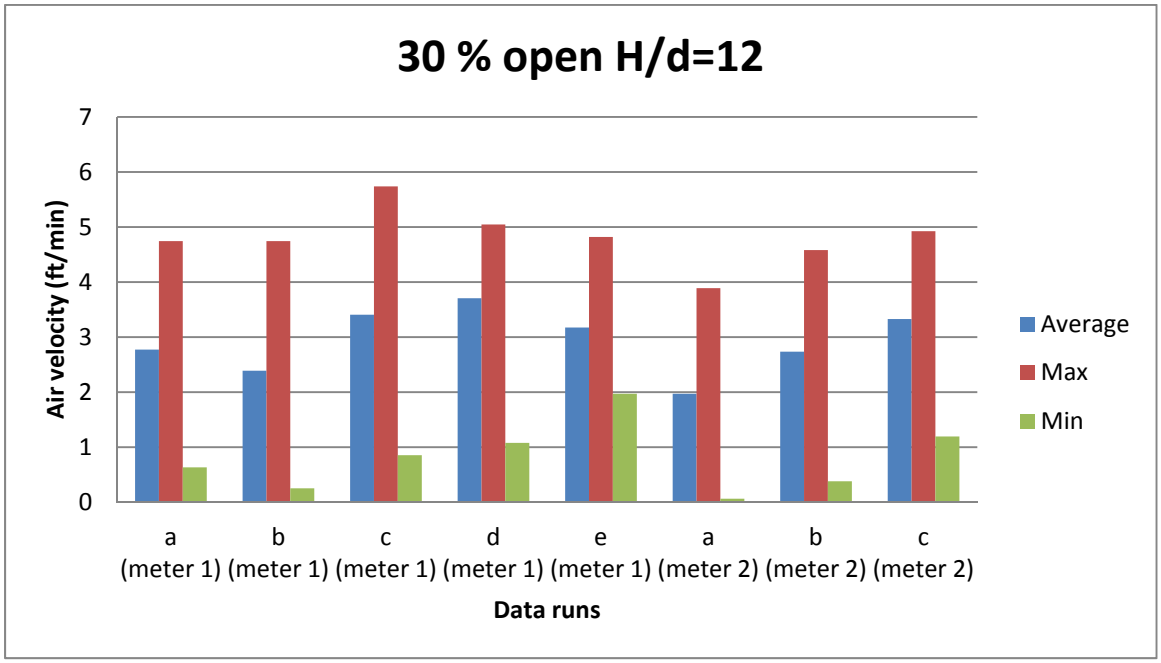

Figure 12. Accuracy experiment 2.

From this experiment, it was determined that the erratic flow observed was due solely to the erratic water flow at such conditions which is consistent with the previous studies demonstrating that the air entrainment in a turbulent, two phased flow environment can be somewhat erratic.

Maximum air demand (based on gate opening)

In an effort to determine the gate opening that resulted in the maximum air demand, a series of tests were performed in which air demand was measured for three minutes at sequential gate openings (i.e., 8 - 100 percent open) while maintaining a constant reservoir head. The results indicated the valve opening at which the peak air demand occurred. For many of the data runs, the peak air flow was observed when the gate was between 50 and 60 percent open as shown in Figure 13. To check consistency,

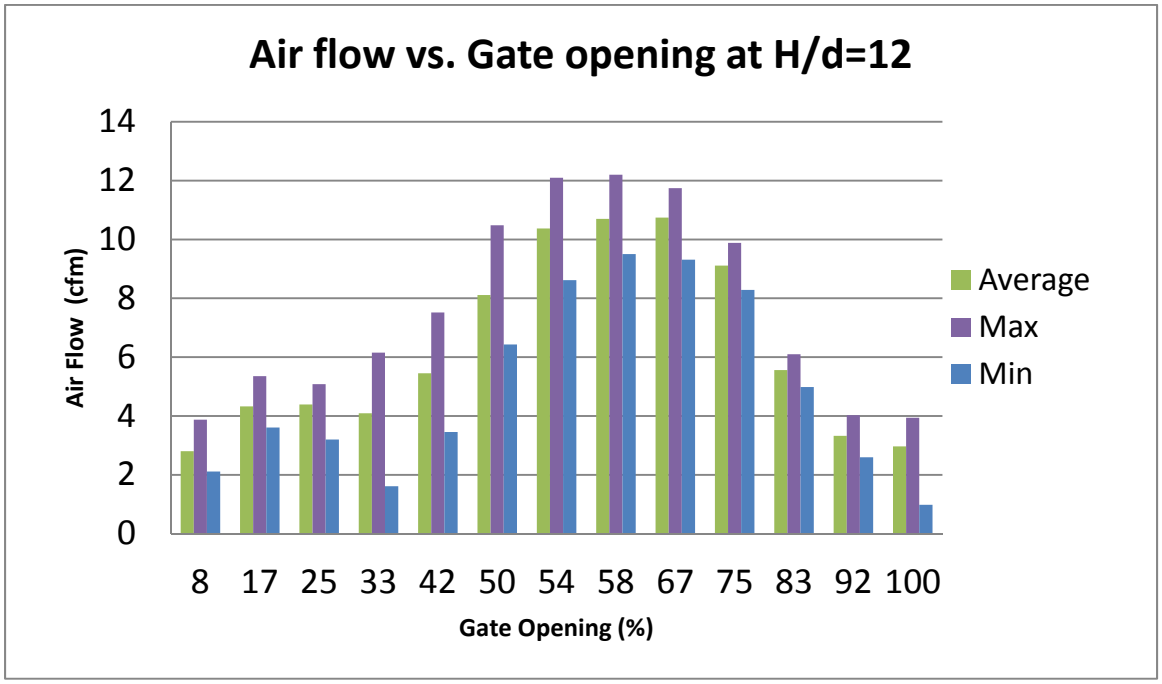

Figure 13. Airflow at H/d=12.

the same test was repeated for H/d = 4, 8, 12, 16, and 20 for both the submerged and non-submerged condition and the results are shown in Appendix B. H/d refers to the driving head in the tank divided by the diameter of the outlet pipe. For water elevations above H/d≥12, the data consistently showed that the maximum air demand occurred between gate openings of 50 and 60 percent.

For heads less than H/d = 12, two maxima occurred; the most apparent at H/d = 4 as seen in Figure 14. The first peak occurred between at gate openings between 20 and 30 percent while the second peak which achieved higher maximum air flow rates was achieved when the gate was close to fully open. At H/d=8 the peak is visible between the range of 58 to 75 percent open as shown in Figure 15.

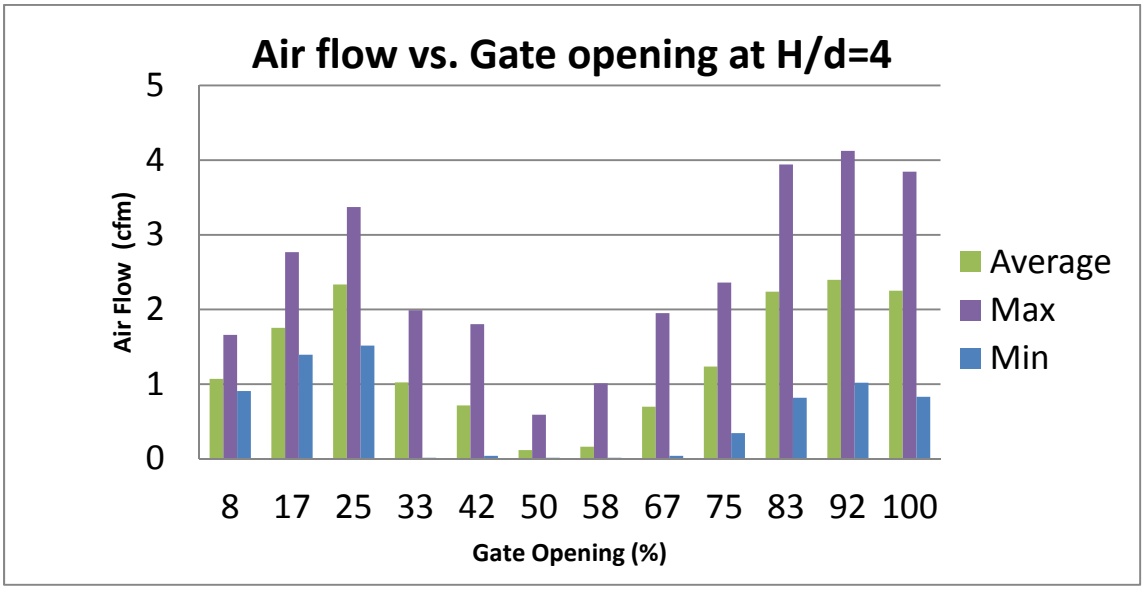

Figure 14. Airflow at H/d=4.

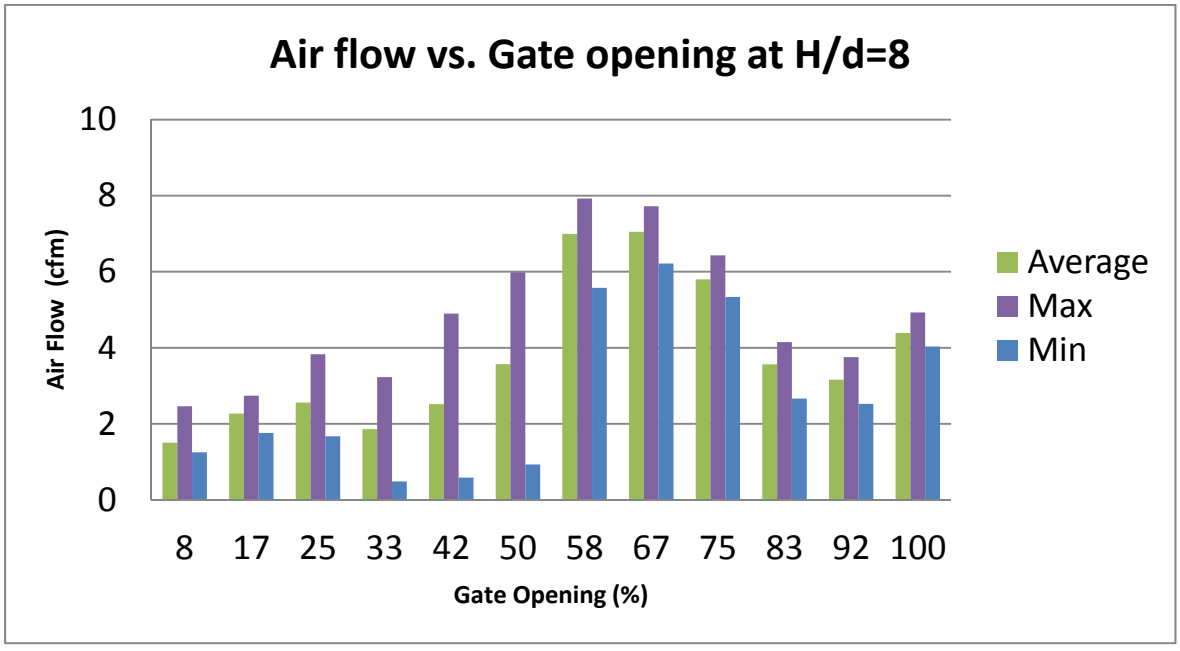

Figure 15. Airflow at H/d=8.

Air demand (based on head in Tank)-free discharge outlet

Data were collected to develop an understanding of the change in air demand as a function of the piezometric head at specific gate openings. After finding that the maximum air demand occurs when the gate was between 50 and 60 percent open, an additional gate opening of 60 percent open was explored to better quantify the air demand for the aforementioned data. Figures 16 and 17 show the average and maximum air demand respectively for various gate openings. As shown, these data also support the previous data illustrating the 50 to 60 percent gate opening results in the maximum air demand for H/d>10.

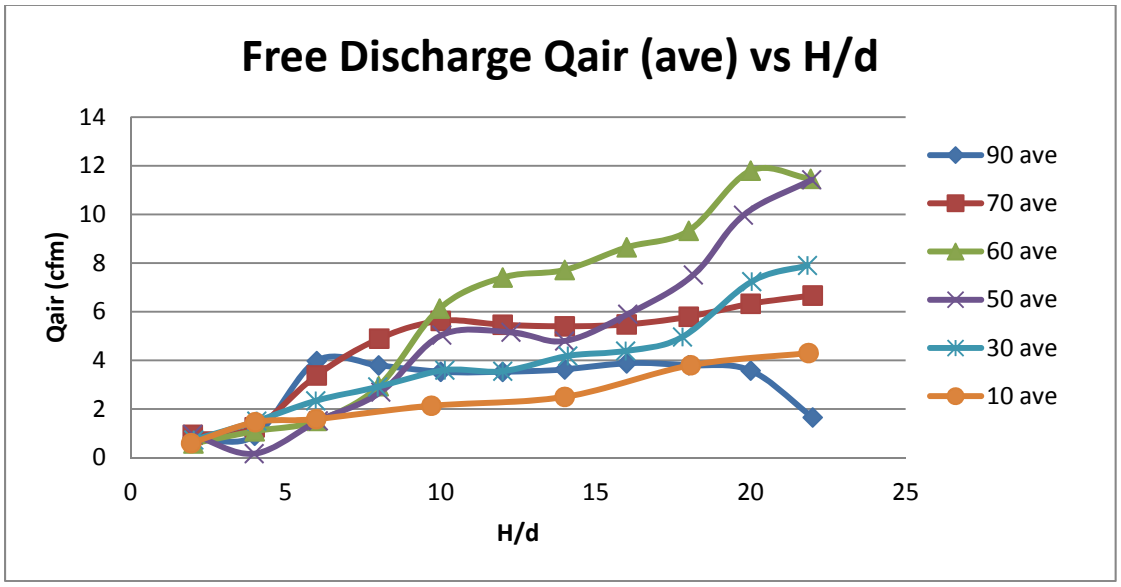

Figure 16. Average air demand for free discharge outlet.

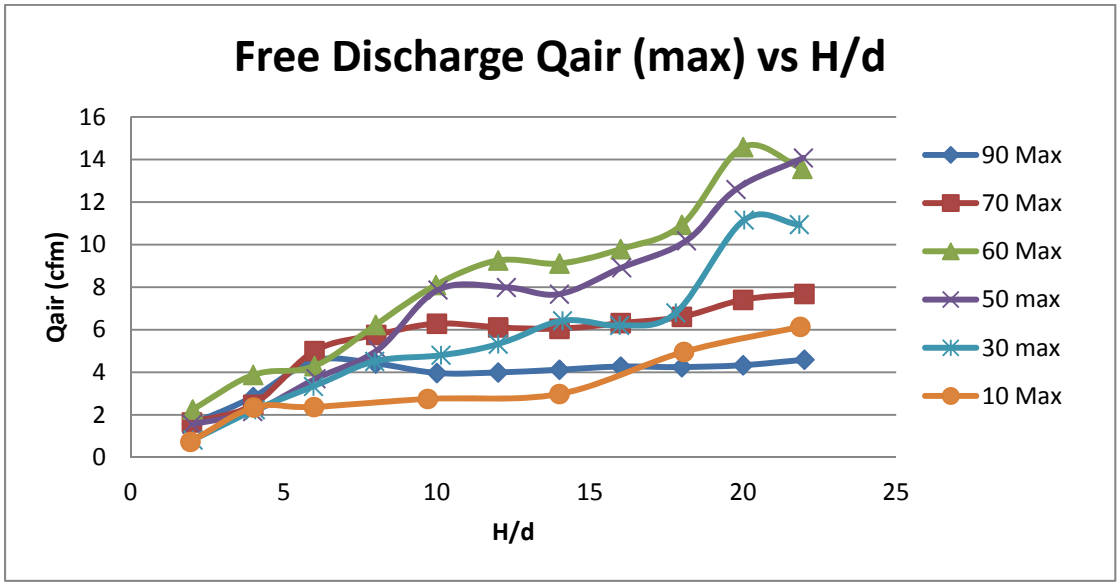

Figure 17. Maximum air demand for free discharge outlet.

For gate openings greater than 60 percent, the air demand decreased due to the increased level of water in the pipe. Especially evident when the gate was 90 percent open, the air demand was significantly less than the 60 percent gate opening. It can also be seen that when the gate was 90% open, there was a very small increase in air demand as the head increased.

Submerged outlet flow air demand

The submerged outlet condition yielded similar results as that of the free discharge condition, however much smaller Q_a values were observed. Figure 18 displays the results of the Q_a data for the submerged outlet. The quantitative difference between the free discharge outlet verses submerged outlet conditions are displayed as a percentage in Table 1. The values shown were calculated by using the following equation:

$$\%\,\text{diff} = \left(1 - \frac{(Q_1 - Q_2)}{Q_1}\right) * 100 \quad (4)$$

where:

Q_1 Average flow rate for the free discharge condition

Q_2 Average flow rate for the submerged condition

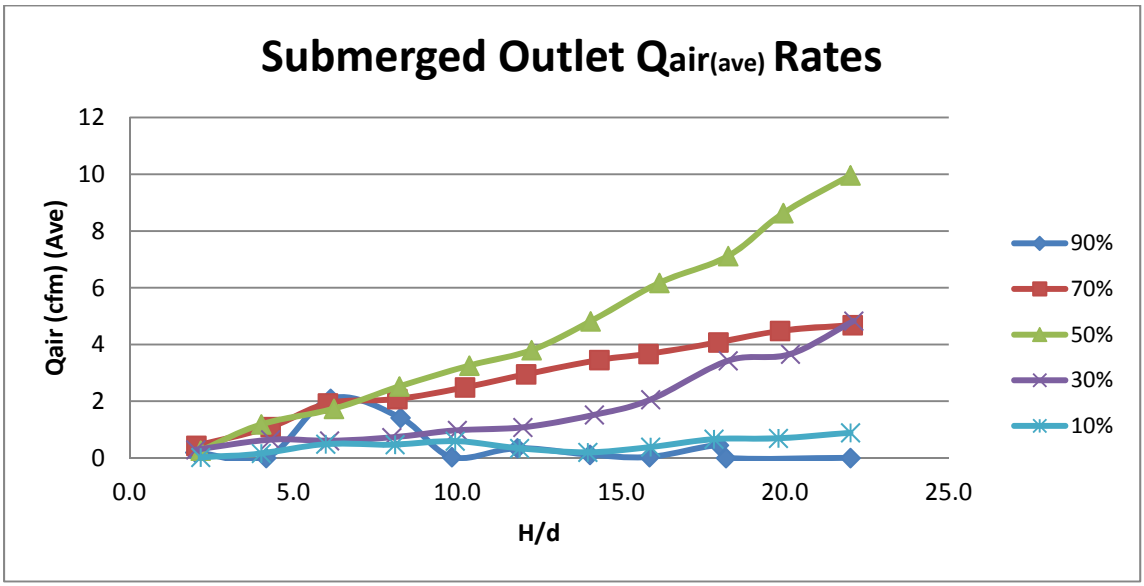

Figure 18. Submerged airflow.

Table 1. % Difference Q_{air} submerged and free discharge.

Q_a (Submerged Outlet) as a percentage of Q_a (Free Discharge Outlet) (Eqn. 4)	
Gate opening (%)	Average difference (%)
90	23.2%
70	61.0%
50	85.2%
30	42.2%
10	18.2%

As shown in Table 1, the Q_a for the submerged outlet condition as a percentage of the air flow for the free discharge condition reached a maximum at a gate opening of 50 percent (maximum air demand case); at which the submerged outlet air demand was 85 percent of non-submerged outlet air demand. For the smaller gate openings it is presumed that more of the air remained in the discharge pipe and was not washed out the end of the pipe as it did in the free discharge case. When the gate was 90 percent open, the flow more readily transitioned to full pipe flow causing an abrupt drop in the average Q_a.

Influence of venting on discharge capacity
(non-submerged condition)

Determining Q_w for the given gate openings was an important part of this research. To date, no published valve discharge coefficients have been found; therefore, estimating flow through such gates is currently difficult. Data were collected in an effort to determine vented and non-vented slide gate discharge coefficients. The submerged outlet and free discharging outlet (both vented condition) Q_w data, compared at the same reservoir head and gate opening, revealed that Q_w passing through the outlet was independent of the tailwater condition. Since the control point for Q_w was the gate (atmospheric pressure boundary condition), any changes downstream had little or no effect on Q_w.

For any non-vented case with tailwater, the flow could be calculated using a form of the Bernoulli equation with the sum of the friction and minor losses (including the gate head loss) being equal to the elevation difference between the head and tailwater. The

resulting Q_w values for the vented and non-vented cases again plotted against H/d are shown in Figure 19 and Figure 20, respectively. Table 2 shows the average percent differences between the vented and non-vented cases. The 10 percent data are not tabulated; this is because the flow in the pipe was open channel flow for both conditions and therefore the Q_w data were the same for each test. It is also important to note that the tabulated data are average values and the percent difference increased with an increase in H/d.

In Figure 19, the last point on the 90 percent curve shows a slight increase in Q_w and is colored orange since it does not follow the pattern of the remainder of the curve. This increase is the result of the change in the flow condition in the pipe from open channel to full pipe flow. Though the air vents remained open, it was observed that at the high head condition Q_a was minimal or equal to zero. This resulted in the Q_w (vented) closer to the Q_w (non-vented). It is worth noting that for such conditions with low aeration req

In Figure 20, it is noticeable that for the 90 and especially the 70 percent open series the flow rates for $H/d \leq 4$, are lower than what would be expected from a curve fit. For these conditions, a vortex formed within the tank introducing air that may be responsible for the decrease in the water flow rate.

uired and full pipe flow, the danger of cavitation is minimal.

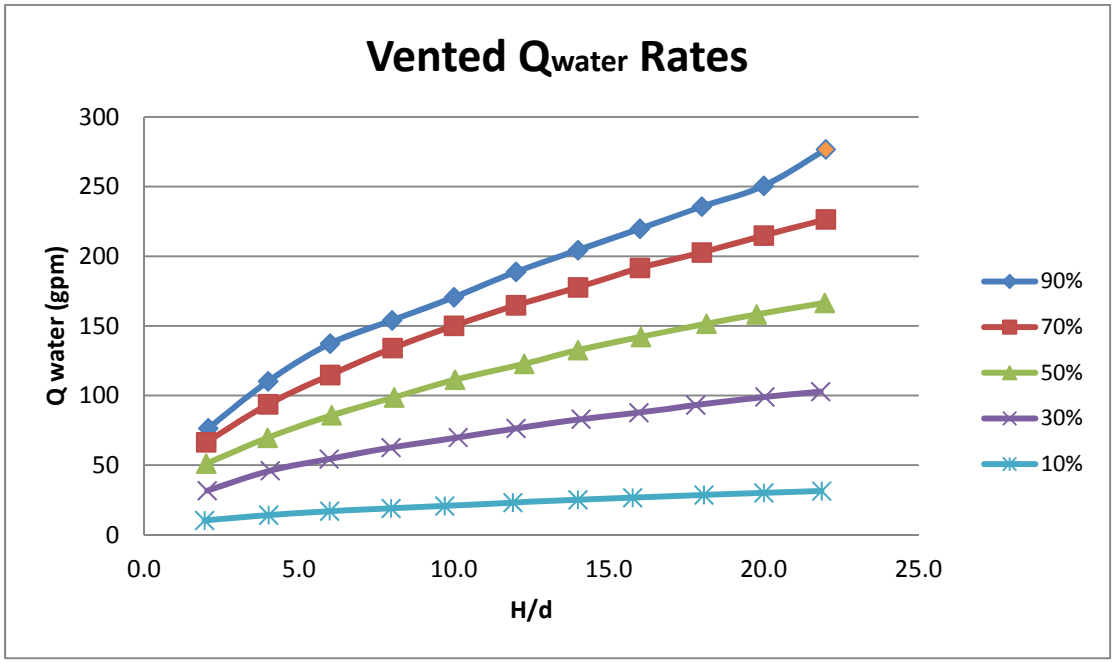

Figure 19. Vented Q_w vs. H/d.

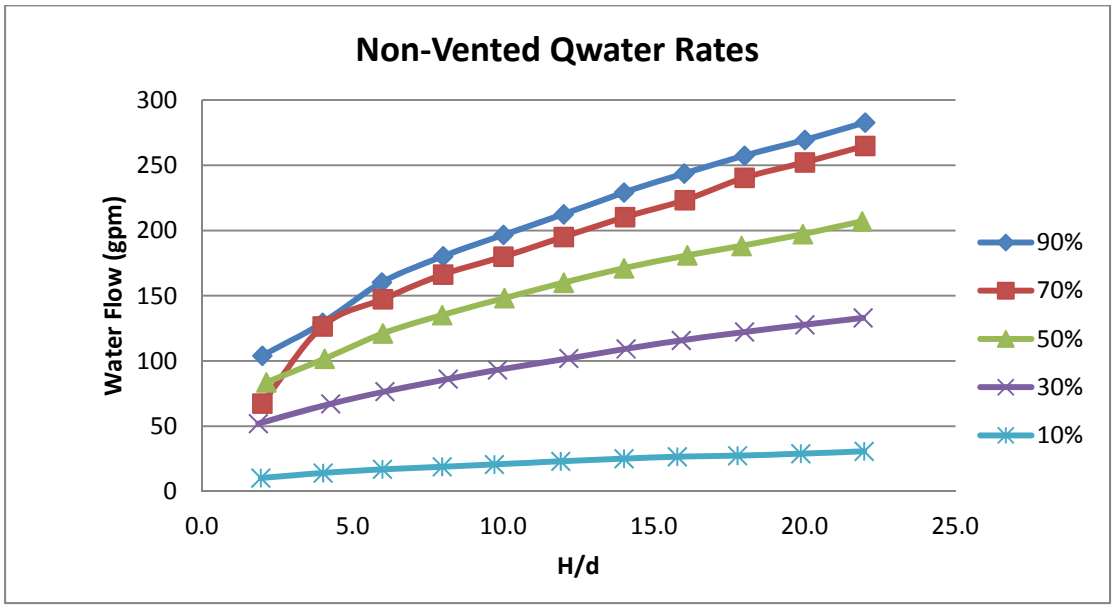

Figure 20. Non-vented Q_w vs. H/d.

Table 2. % Reduction in Q_w by venting.

% Reduction in Flow Caused by Venting	
Gate opening (%)	Average Reduction (%)
90	12%
70	20%
50	35%
30	37%

Valve Discharge Coefficients:

Using the water discharge data from the preceding section, the C_d values were calculated for the slide gate (see Appendix C for calculation steps). Two sets of coefficients are presented in this research corresponding to the flow rates discussed previously: vented and non-vented cases.

The resulting coefficients are displayed in Figures 21 through 23. Figures 21 and 22 show C_d values calculated for each gate opening for the non-vented and vented condition, respectively, while Figure 23 shows the average C_d values for each gate opening plotted in a single curve. Also noticeable in Figure 21 is the limited points of data for the 10 percent open series of the data. Below H/d=16 the flow in the pipe was open channel creating a "vented" condition downstream of the slide gate. See Figure 22 for the ten percent gate opening C_d data for $H/d < 16$. Figures 22 and 23 show the same data as discussed here, but for the vented condition.

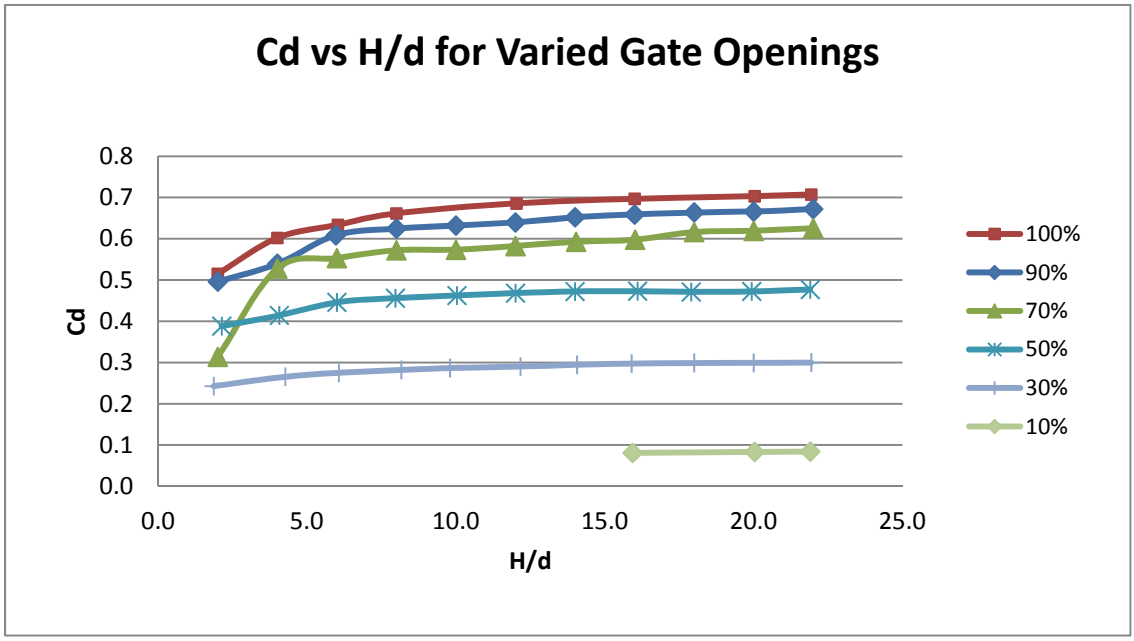

Figure 21. Slide gate C_d values (non-vented).

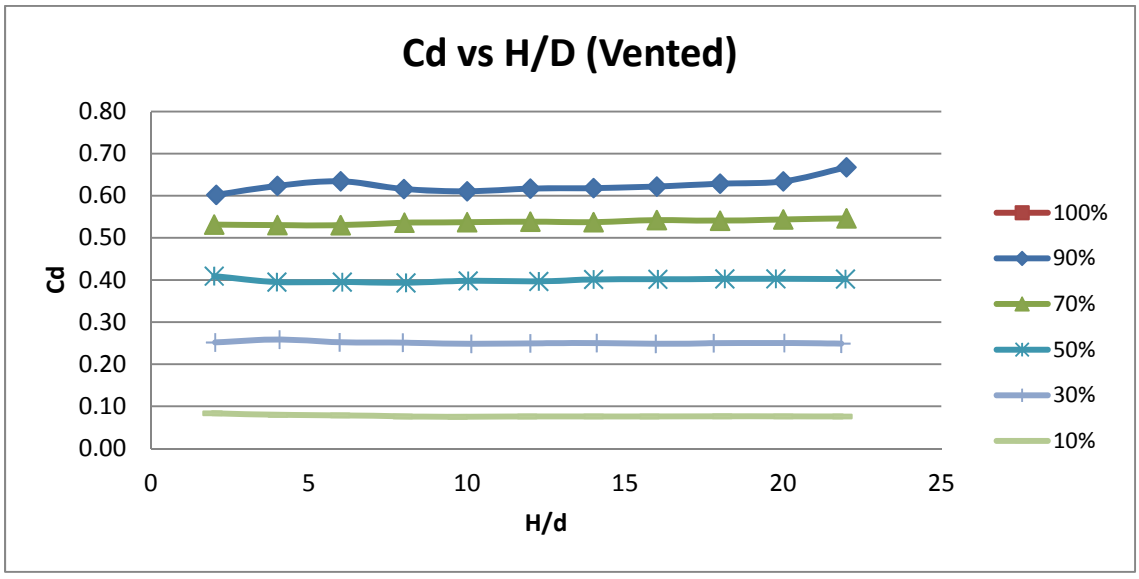

Figure 22. Slide gate C_d values (vented).

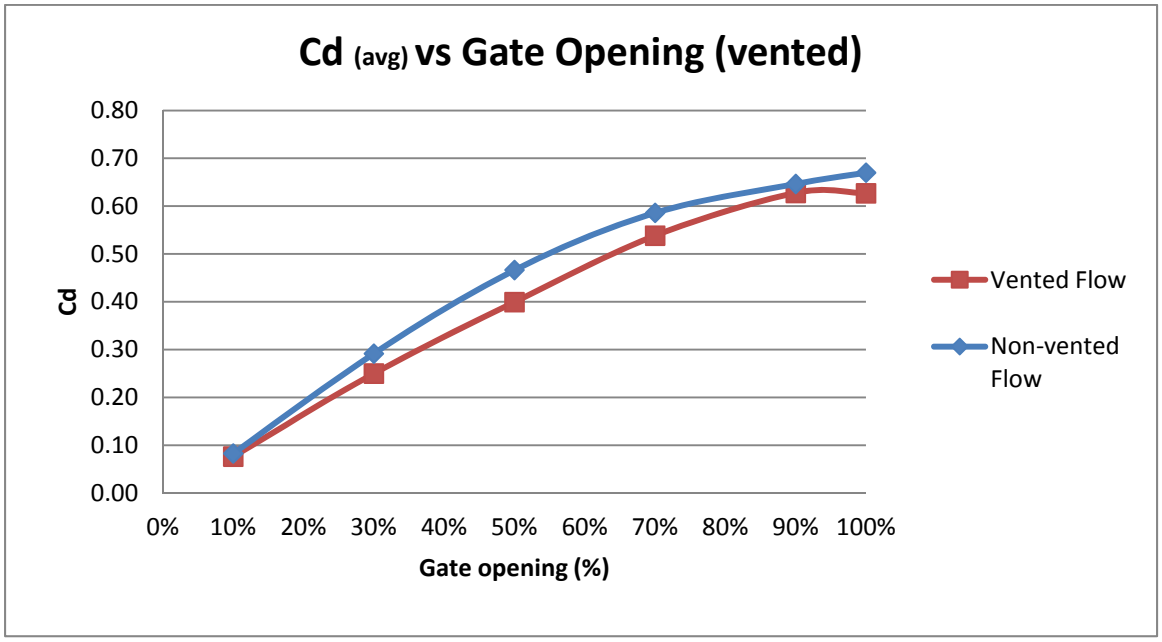

Figure 23. Slide gate average C_d values vs. gate opening.

Negative pressure

The magnitude of the negative pressures were measured for the non-vented condition but were not used for any calculations. The pressure was measured as described in Chapter 3 and converted to psi. Figure 24 shows the magnitude of the negative pressures that developed. Though the measurements approached the lower limits of the vacuum gauge, the negative pressures have a mostly linear relationship with an increase in driving head. As previously discussed, the air demand for the 90 percent open gate was minimal. The pressure data below supports the previous data in showing a pressure of zero that would consequently result in a low air demand.

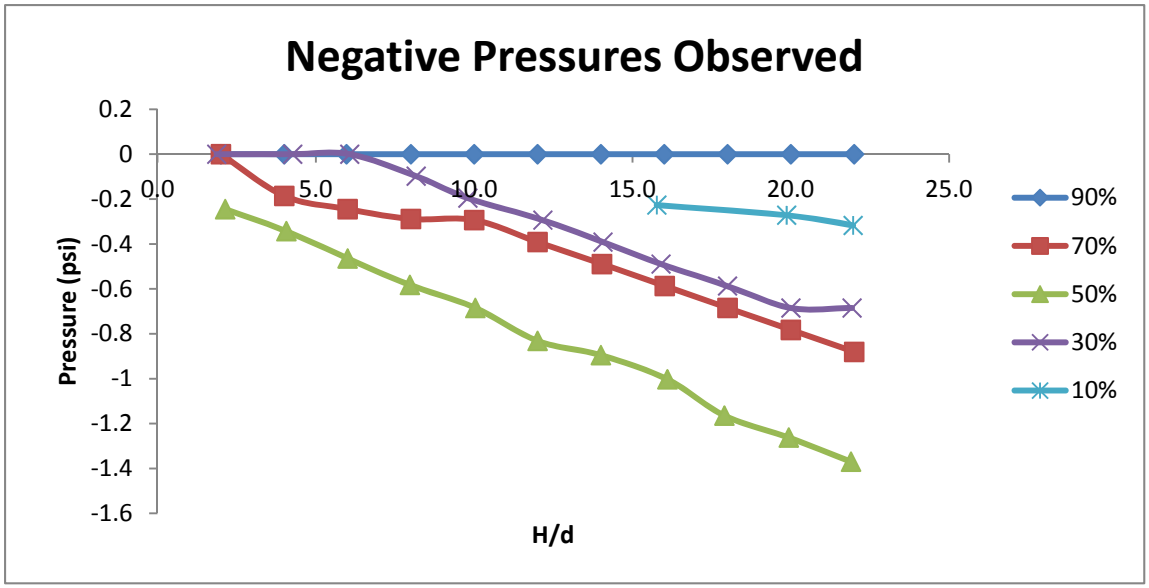

Figure 24. Negative pressures.

Flow conditions observed

An effort was made to note specific conditions that existed in the pipe flow or in the tank itself. The existence of vortices especially was noted. Figure 25 shows Q_w plotted as before, but the shaded area represents conditions where vortices were present (continuously or intermittent). Vortex formation in the model was manifest in Q_w values as well as Q_a . When vortices existed, they served as an additional source of air, and reduced the net area of water flow causing a decrease in the water flow. This is evident in Figure 20 for the 70 and 90 percent open gate openings where the $H/d < 2$.

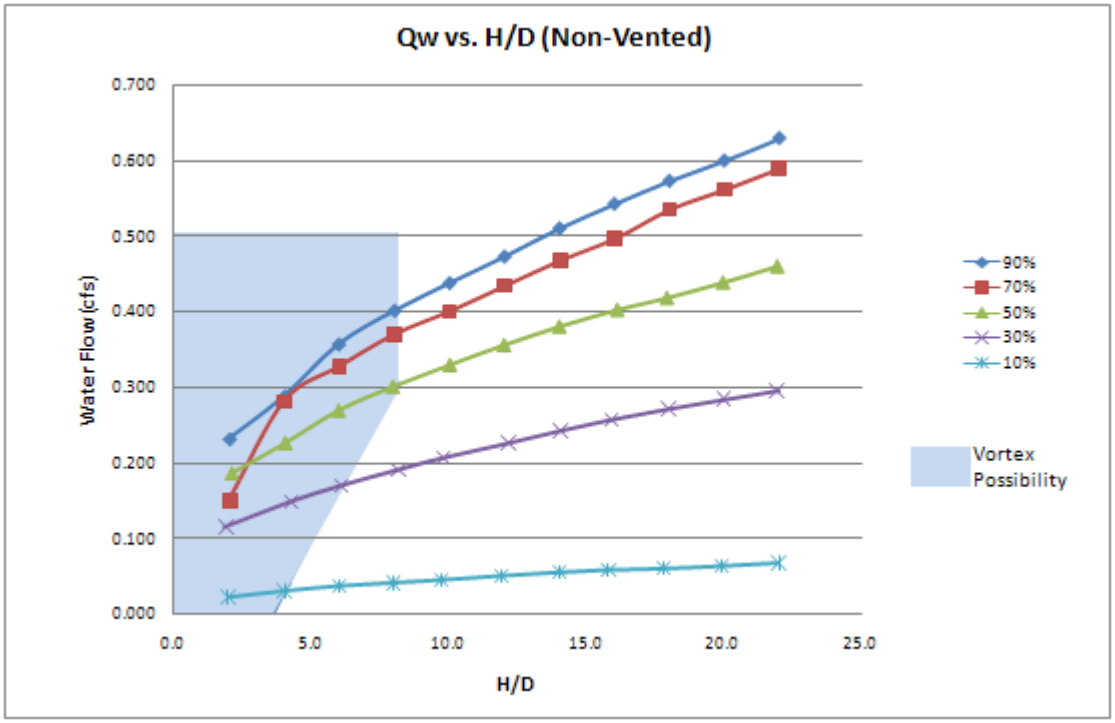

Figure 25. Vortex possibilities.

Beta values (Q_a/Q_w)

Air demand is commonly represented dimensionlessly as the ratio of $\beta = Q_a/Q_w$. The average and maximum β values are presented in Figures 26 and 27 which correspond to the average and maximum values of Q_a for the free discharge condition. The average Q_a are simply the total average of the sample. The maximum Q_a, that are also used in the β ratios, was the maximum value recorded during a sample. Similar results from the submerged flow are shown in Figures 28 and 29 for comparison.

When analyzing the values for β, it is imperative to keep the proper perspective on what is really displayed. At first glance β can be misleading; the 10 percent open gate produced the highest β values, but the 50 – 60 percent gate opening results in the largest

volumetric air demand as demonstrated clearly in Figure 28. Design should be based on the largest air demand rather than β. At the gate opening of 10 percent the water flow rate is very small causing the ratio of Q_a/Q_w to be very large.

With C_d and β ratio values, it is possible to estimate an air vent diameter if a design velocity is specified for the vent. Of course, if there are any size scale effects, at this point they are ignored, and there is much research yet to be done on the subject, but a basic design method can be developed from the data obtained and a step-by-step example is discussed in Chapter 5.

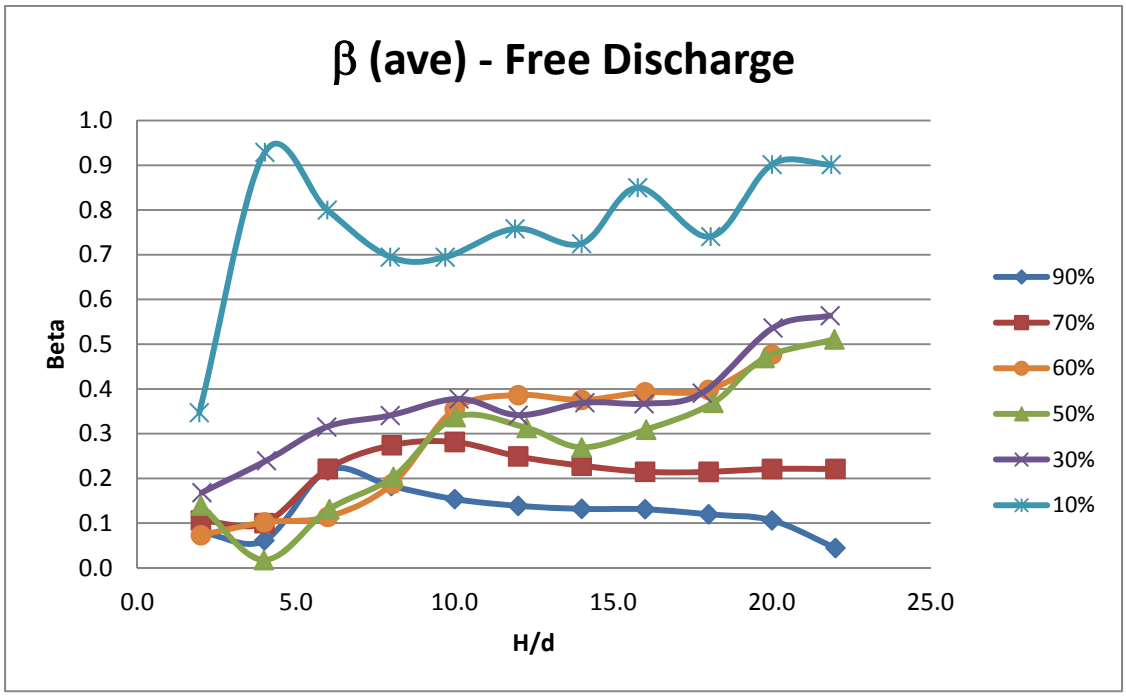

Figure 26. Average β - (free discharge).

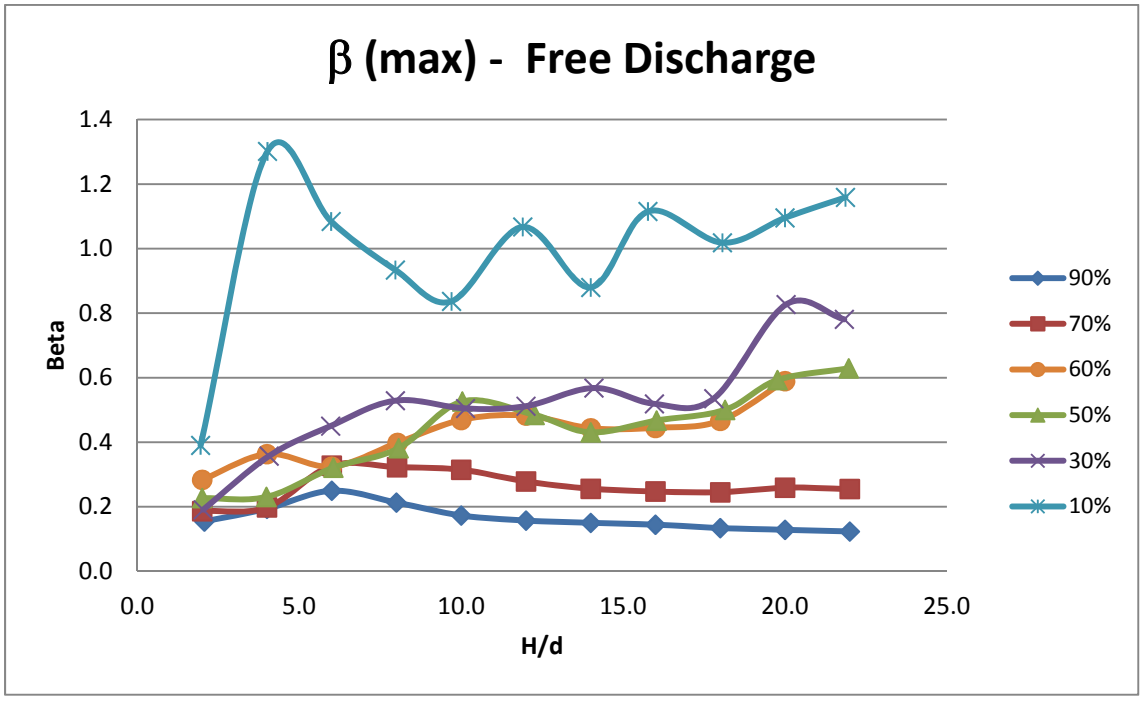

Figure 27. Max β – (free discharge).

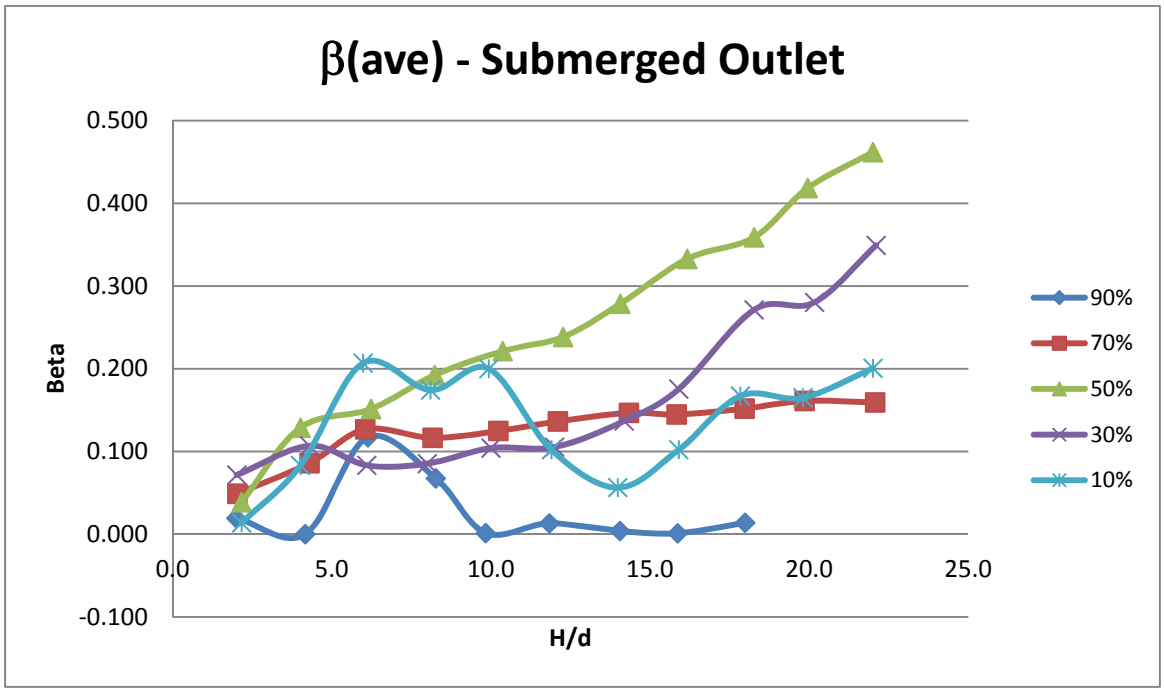

Figure 28. Average β - submerged outlet.

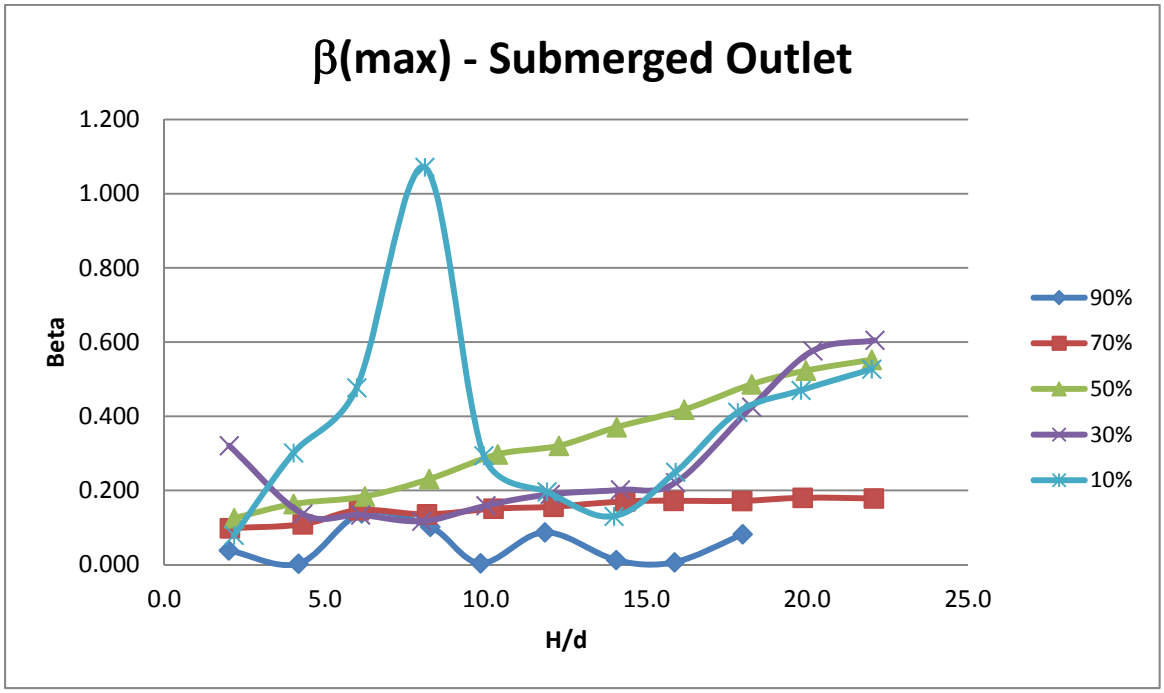

Figure 29. Max - submerged outlet.

CHAPTER 5

APPLICATION OF RESEARCH EXAMPLE

The purpose of this research was to better estimate the size required for adequate air venting in small dams. The following is one possible method of sizing air vents based on this research. For design purposes, it is suggested to design for the worst-case scenario possible for a given dam (i.e., highest head and 50-60 percent open gate). For the design example to follow, the maximum β values will be used, which is a more conservative method. After calculating the vent size a factor of safety may also be added. The following is a hypothetical example of the design procedure with the limitations as indicated.

A given set of parameters will be assumed as follows:

Head in Reservoir	20 ft
Gate opening	50 % open
Gate and Pipe Diameter	24 in

The following are assumed to be constants or design criteria:

g (acceleration due to gravity)	32.17 ft/s^2
Air Velocity (maximum)	100 ft/s
$Area_{(pipe)}$	3.14 ft^2 (calculated from diameter)

Solution:

1. Obtain a value for C_d from Figure 23. (C_d=0.4 for H/d=10)
2. By drawing in a design envelope in Figure 27 as shown in Figure 30 we can obtain a value for β. (β=0.5 for H/d=10)

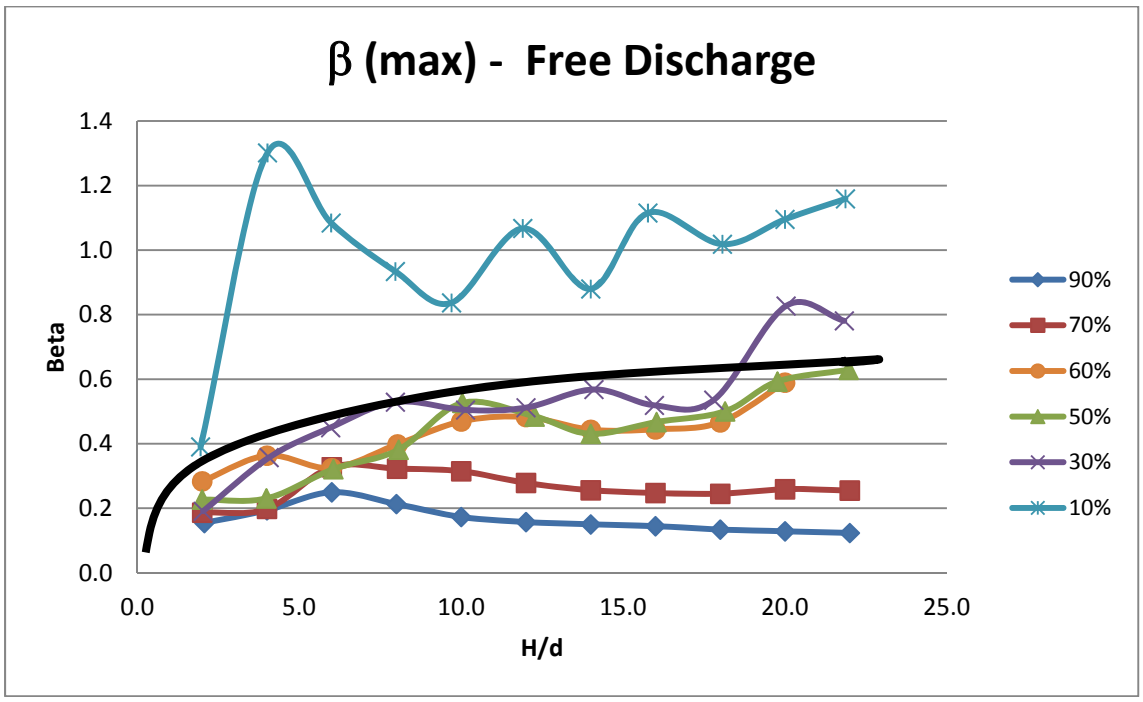

Figure 30. Design envelope.

3. Calculate K by re-arranging Equation 11 (Appendix C) as follows:

$$K = \frac{1}{C_d^{\,2}} - 1 \qquad \text{(K=5.25)} \tag{5}$$

4. Calculate flow through the dam using K from Step 3, and by re-arranging Equation 1 as follows.

$$Q = \left(\frac{\Delta H * 2gA^2}{K} \right)^{0.5} \quad \text{(Q=49.2 cfs)} \tag{6}$$

5. Calculate Q_a by multiplying $\beta * Q_{w.}$ (Q_a = 24.6 cfs)
6. Calculate the area required for the air vent by limiting the velocity to 100 fps and using the equation Q=VA. (A_{req}=.25 ft^2)
7. Calculate the diameter of the air pipe using the following equation:

$$D_{Air} = \left(\frac{4 * A/144}{\pi} \right)^{0.5} \quad (D_{Air}=6.7 \text{ in.}) \tag{7}$$

8. Multiply by factor of safety (user defined).

   If FS=1.2 the air pipe needs to be 8 inches. (8.06 in.)

   If FS=1.5 the air pipe needs to be 10 inches. (10.07 in.)

Note that this design method/example ignores the influence of air flow resistance/energy loss in the vent pipe. If appreciable head loss exists, this should be accounted for, resulting in a larger vent pipe diameter requirement for a give Q_a requirement.

CHAPTER 6

CONCLUSIONS

This research presents the estimation of air demand for low-level small to medium sized embankment dam outlet works featuring an inclined slide gate followed by a elbow and conduit. Since the geometry of the outlet works differs so much from that of large dams, the traditional methods of estimating air demand could not be used. A scaled laboratory model was constructed and the results have been discussed. Based on the results of this study, the following conclusions have been made.

1. Air demand has been determined to be a function of several variables, however this study was limited to examining the air demand as a function of driving head and gate opening only. The experiments showed that the air flow may be very erratic at certain gate openings and very steady for other conditions. Typically, the air flow is more steady and constant for low heads ($H/d < 12$) and small gate openings. Erratic flow was observed during the majority of the experiments and was closely linked to the turbulence of the water flow.
2. The gate opening resulting in the maximum air demand occurs between 50 and 60 percent for $H/d \geq 12$. For $H/d \leq 12$ the gate opening causing the maximum air demand varied but approached the gate opening of 100 percent with decreasing head.

3. The negative pressure behind the gate has a linear relationship with H/d. Though the pressures were observed to be linear, the air flow measured did not follow the same trend and was often erratic and non-repeatable.
4. Surface vortex formation was observed for $H/d \leq 8$ for many of the data experiments. The main effect of the vortices observed was a decrease in the efficiency of the water flow thus affecting the C_d values.
5. With the collection of water flow rates through the outlet works it was possible to calculate C_d values for a typical circular gate that can be used to calculate water flow through a geometrically similar gate. Water masters and dam operators will be able to use this data to better calculate discharge through the dams in the absence of metering devices and more applicable data.
6. With the graphs including C_d and β values, a suitable method has been developed to estimate the size for air vents for $H/d \leq 22$. C_d values can be obtained from the data, as well as values for β for a given H/d. With this information, and defining a maximum air velocity in the air vent, an air vent can be sized following the steps in Chapter 6.

Topics not included in this research that would be of benefit for future studies include:

1. Scale effects. Methods for scaling the air flows observed in the laboratory data have not been tested with additional sizes. Additional scaled models

should be tested to determine if scale effects exist. Also, these results could be compared to prototype data.

2. Gate designs. In this research, only one gate design was examined. Additional common designs and associated effects on air flow and water flow would be beneficial.
3. Tests investigating any effects from changes in the conduit slope or length.
4. Air venting collars. Many dams have an air vent collar around the pipe downstream of the slide gate. Though it was determined that the air demand was satisfied in this research, the effects of such collars were not explored.

REFERENCES

Dettmers, D., 1953. "Beitrag zur Frage der Belüftung von Tiefschützen (A Contribution to the problem of aeration of deep outlet gates)", Mitteilung der Versuchsanstalt für Grund u. Wasserbau der Technischen Hochschule, Hannover, H-4.

Falvey, H. T. 1980. Air-water flow in hydraulic structures. Engineering Monograph 41. U.S. Department of the Interior, Water and Power Resources Service, Denver, Colorado. 160 p.

Kalinske, A. A., and J. W. Robertson. 1943. Closed conduit flow. ASCE Transactions 108: 1435-1447.

Sharma, H.R. 1976. Air-entrainment in high head gated conduits. ASCE Journal of the Hydraulics Division 102(HY 11): 1629–1646.

Speerli, J. 1999. Air entrainment of free-surface tunnel flow. Proceedings of the 28th IAHR Congress, Graz, Austria.

Speerli, J., Willi H. 2000. Air-water flow in bottom outlets. Canadian Journal of Civil Engineering 27, 454-462.

Tullis, J. Paul. 1989. Hydraulics of pipelines. John Wiley and Sons, Inc., Canada. 266 p.

USACE (United States Army Corps of Engineers). 1980. Hydraulic design of reservoir outlet works. Engineer Manual 1110-2-1602.

USBR (United States Bureau of Reclamation). 1966. Hydraulic model studies of the Silver Jack Outlet Works Bypass, Bostwick Park Project, Denver, Colorado. 21 p.

APPENDICES

Appendix A: Visual Basic Programming

Orifice Meter Calibration

Flow metering for the physical model was accomplished using orifice meters calibrated at the UWRL. Standard methods were used in the calibration of the orifice plates installed in the 4-in. supply line and the 2-in. supply line. The calibration and Visual Basic programming for each are shown in Figures 31 and 32.

```
'4 inch orifice 3' flume 2/28/2008
If key = "4inMHg" Then
  dh = (cm * 0.032808) * (sgHG - 1)
    Apipe = WorksheetFunction.Pi() * (4.026 / 12) ^ 2 / 4
    Athr = WorksheetFunction.Pi() * (3 / 12) ^ 2 / 4
    B = 3 / 4.026
    Q = 0.6296 * Athr * Sqr((64.34 * dh) / (1 - B ^ 4))
    re = Q / Apipe * (4.026 / 12) / kv
    c1 = 0.6296
    dif = 1
    Do While Abs(dif) > 0.00001
        c2 = 5.66037E-12 * re ^ (2) - 0.00000078798 * re + 0.657473
        If re >= 66349 Then c2 = 0.6927513 * re ^ -0.0084973
        Q = c2 * Athr * Sqr((64.34 * dh) / (1 - B ^ 4))
        re = Q / Apipe * (4.026 / 12) / kv
        dif = c2 - c1
        c1 = c2
    Loop
    Flow1 = c1 * Athr * Sqr((64.34 * dh) / (1 - B ^ 4)) * 448.831
End If
```

Figure 31. 4-in. orifice calibration

```
'2" line East of 3' flume
If key = "2inHg" Then '2-inch orifice 12/03 revised 12/04 because of roundoff errors
 dh = (cm * 0.032808) * (sgHG - 1)
  B = 1.127 / 2.067
  Q = 0.625 * 0.0069274790547 * Sqr((64.34 * dh) / (1 - B ^ 4))
  re = Q / 0.023302812595 * (2.067 / 12) / kv
  c1 = 0.625
  dif = 1
  Do While Abs(dif) > 0.001
     c2 = -0.0263 * (re / 10000) ^ 3 + 0.1023 * (re / 10000) ^ 2 - 0.1349 * (re / 10000) + 0.6842
     If re >= 12382 Then c2 = -0.0005 * (re / 10000) + 0.6247
     Q = c2 * 0.0069274790547 * Sqr((64.34 * dh) / (1 - B ^ 4))
     re = Q / 0.023302812595 * (2.067 / 12) / kv
     dif = c2 - c1
     c1 = c2
  Loop
 Flow1 = c1 * 0.0069274790547 * Sqr((64.34 * dh) / (1 - B ^ 4)) * 448.831
End If
```

Figure 32. 2-in. orifice calibration

Appendix B: Experimental Data

Free Discharge - Vented

90%	Head (H - ft)	Flow (gpm)	H/D	Q_{Air} (Avg)	Q_{Air} (Max)	Cd	KL
	0.52	76.49	2.07	0.81	1.58	0.63	1.76
	1.00	110.19	4.00	0.90	2.85	0.65	1.57
	1.50	137.30	6.00	4.00	4.58	0.66	1.49
	2.00	153.95	8.00	3.77	4.39	0.64	1.64
	2.50	170.61	10.00	3.51	3.94	0.63	1.68
	3.00	188.85	12.00	3.50	3.97	0.64	1.63
	3.50	204.37	14.00	3.60	4.10	0.64	1.62
	4.00	219.78	16.00	3.85	4.24	0.65	1.59
	4.50	235.70	18.00	3.78	4.22	0.65	1.53
	5.00	250.60	20.00	3.56	4.31	0.66	1.49
	5.50	276.67	22.00	1.64	4.56	0.69	1.24

70%	Head (H - ft)	Flow (gpm)	H/D	Q_{Air} (Avg)	Q_{Air} (Max)	KL	Cd
	0.50	66.43	2.00	0.94	1.66	0.66	2.54
	1.00	93.73	4.00	1.25	2.48	0.65	2.55
	1.50	114.76	6.00	3.40	5.02	0.65	2.56
	2.00	134.11	8.02	4.92	5.78	0.66	2.48
	2.50	150.10	10.00	5.65	6.32	0.66	2.47
	3.00	164.85	12.00	5.49	6.14	0.67	2.45
	3.50	177.64	14.00	5.42	6.08	0.66	2.46
	4.00	191.67	16.00	5.50	6.34	0.67	2.40
	4.50	202.74	18.00	5.82	6.64	0.67	2.42
	5.00	214.93	20.00	6.35	7.44	0.67	2.38
	5.50	226.46	22.00	6.70	7.72	0.67	2.35

60%	Head (H - ft)	Flow (gpm)	H/D	Q_{Air} (Avg)	Q_{Air} (Max)	KL	Cd
	0.51	59.49	2.00	0.58	2.25	No Data	
	1.00	79.90	4.00	1.09	3.88	No Data	
	1.50	99.11	6.00	1.51	4.30	No Data	
	2.00	117.09	8.03	2.94	6.23	No Data	
	2.49	129.30	10.00	6.13	8.10	No Data	
	3.00	143.46	12.00	7.41	9.26	No Data	
	3.50	153.84	14.00	7.72	9.12	No Data	
	4.00	164.85	16.00	8.65	9.79	No Data	
	4.50	175.40	18.00	9.33	10.93	No Data	
	5.00	185.12	20.00	11.80	14.59	No Data	

Free Discharge - Vented

50%	Head (H - ft)	Flow (gpm)	H/D	Q_{Air} (Avg)	Q_{Air} (Max)	KL	Cd
	0.50	51.13	2.00	0.95	1.55	0.68	4.97
	1.00	69.66	3.98	0.16	2.15	0.65	5.41
	1.51	85.84	6.05	1.51	3.69	0.65	5.41
	2.02	98.68	8.07	2.68	5.03	0.65	5.47
	2.51	111.37	10.03	5.02	7.84	0.66	5.32
	3.07	122.74	12.27	5.13	7.95	0.66	5.36
	3.50	132.68	14.00	4.78	7.64	0.66	5.21
	4.01	142.10	16.03	5.87	8.87	0.66	5.20
	4.54	151.55	18.15	7.48	10.14	0.67	5.17
	4.94	158.22	19.77	9.92	12.54	0.67	5.16
	5.49	166.56	21.97	11.37	14.01	0.67	5.18

30%	Head (H - ft)	Flow (gpm)	H/D	Q_{Air} (Avg)	Q_{Air} (Max)	KL	Cd
	0.51	31.71	2.03	0.71	0.81	0.68	14.79
	1.02	46.06	4.07	1.47	2.20	0.70	13.96
	1.49	54.41	5.97	2.29	3.27	0.68	14.74
	1.99	62.64	7.97	2.85	4.43	0.68	14.85
	2.53	69.87	10.13	3.53	4.71	0.67	15.21
	3.00	76.39	12.00	3.48	5.23	0.68	15.05
	3.53	83.03	14.10	4.10	6.31	0.68	14.97
	3.99	87.71	15.97	4.30	6.08	0.67	15.21
	4.45	93.18	17.80	4.87	6.67	0.68	15.01
	5.01	98.99	20.03	7.10	10.94	0.68	14.96
	5.46	102.83	21.83	7.75	10.73	0.68	15.12

10%	Head (H - ft)	Flow (gpm)	H/D	Q_{Air} (Avg)	Q_{Air} (Max)	KL	Cd
	0.49	10.30	1.95	0.48	0.54	0.72	142.54
	1.00	14.10	4.02	1.75	2.45	0.68	156.72
	1.50	17.01	5.98	1.82	2.47	0.68	160.40
	1.99	18.94	7.97	1.76	2.36	0.65	172.35
	2.43	20.69	9.70	1.92	2.31	0.65	175.89
	2.98	23.13	11.90	2.34	3.30	0.65	172.63
	3.50	25.16	14.00	2.44	2.96	0.65	171.62
	3.94	26.64	15.77	3.03	3.97	0.65	172.51
	4.52	28.61	18.07	2.83	3.89	0.65	171.29
	5.00	30.10	20.00	3.63	4.41	0.65	171.38
	5.47	31.43	21.87	3.79	4.87	0.65	171.88

Free Discharge - Non Vented

90%	Head (H - ft)	Flow (gpm)	H/D	KL	Cd	Negative Pressure
	0.50	104.0	2.0	3.06	0.50	0
	1.00	129.3	4.0	2.43	0.54	0
	1.49	160.2	6.0	1.70	0.61	0
	2.00	180.3	8.0	1.56	0.62	0
	2.50	196.7	10.0	1.50	0.63	0
	3.00	212.4	12.0	1.44	0.64	0
	3.50	229.2	14.0	1.35	0.65	0
	4.00	243.7	16.0	1.30	0.66	0
	4.50	257.4	18.0	1.27	0.66	0
	5.00	269.4	20.0	1.26	0.67	0
	5.50	282.8	22.0	1.21	0.67	0

70%	Head (H - ft)	Flow (gpm)	H/D	KL	Cd	Negative Pressure
	0.50	67.4	2.0	9.16	0.31	0
	1.00	126.5	4.0	2.59	0.53	-0.19
	1.50	147.4	6.0	2.27	0.55	-0.24
	2.00	166.3	8.0	2.06	0.57	-0.29
	2.50	179.9	10.0	2.04	0.57	-0.29
	3.00	195.0	12.0	1.95	0.58	-0.39
	3.51	210.3	14.0	1.85	0.59	-0.49
	4.00	223.2	16.0	1.80	0.60	-0.59
	4.50	240.5	18.0	1.63	0.62	-0.68
	5.00	252.3	20.0	1.61	0.62	-0.78
	5.50	264.9	22.0	1.56	0.63	-0.88

50%	Head (H - ft)	Flow (gpm)	H/D	KL	Cd	Negative Pressure
	0.53	83.6	2.1	5.63	0.39	-0.24
	1.02	101.7	4.1	4.82	0.41	-0.34
	1.50	121.1	6.0	4.03	0.45	-0.46
	1.99	135.2	8.0	3.81	0.46	-0.58
	2.51	148.2	10.0	3.68	0.46	-0.68
	3.00	160.0	12.0	3.56	0.47	-0.83
	3.50	171.0	14.0	3.49	0.47	-0.90
	4.03	181.0	16.1	3.47	0.47	-1.00
	4.48	188.2	17.9	3.51	0.47	-1.16
	4.98	197.2	19.9	3.48	0.47	-1.26
	5.48	207.0	21.9	3.40	0.48	-1.37

Free Discharge - Non Vented

30%	Head (H - ft)	Flow (gpm)	H/D	KL	Cd	Negative Pressure
	0.47	52.0	1.9	15.97	0.24	0.00
	1.07	67.2	4.3	13.18	0.27	0.00
	1.52	76.6	6.1	12.22	0.28	0.00
	2.04	86.2	8.2	11.57	0.28	-0.10
	2.45	93.2	9.8	11.17	0.29	-0.20
	3.04	102.0	12.2	10.87	0.29	-0.29
	3.52	109.3	14.1	10.52	0.29	-0.39
	3.98	115.8	15.9	10.29	0.30	-0.49
	4.50	122.3	18.0	10.18	0.30	-0.59
	5.00	127.8	20.0	10.17	0.30	-0.68
	5.48	133.1	21.9	10.12	0.30	-0.68

10%	Head (H - ft)	Flow (gpm)	H/D	KL	Cd	Negative Pressure
	0.49	10.3	2.0	No Data		No Data
	1.00	14.1	4.0	No Data		No Data
	1.50	17.0	6.0	No Data		No Data
	1.99	18.9	8.0	No Data		No Data
	2.43	20.7	9.7	No Data		No Data
	2.98	23.1	11.9	No Data		No Data
	3.50	25.2	14.0	No Data		No Data
	3.94	26.6	15.8	151.86	0.08	-0.23
	4.44	27.4	17.8	No Data		No Data
	4.97	29.0	19.9	143.25	0.08	-0.27
	5.49	30.8	22.0	140.29	0.08	-0.32

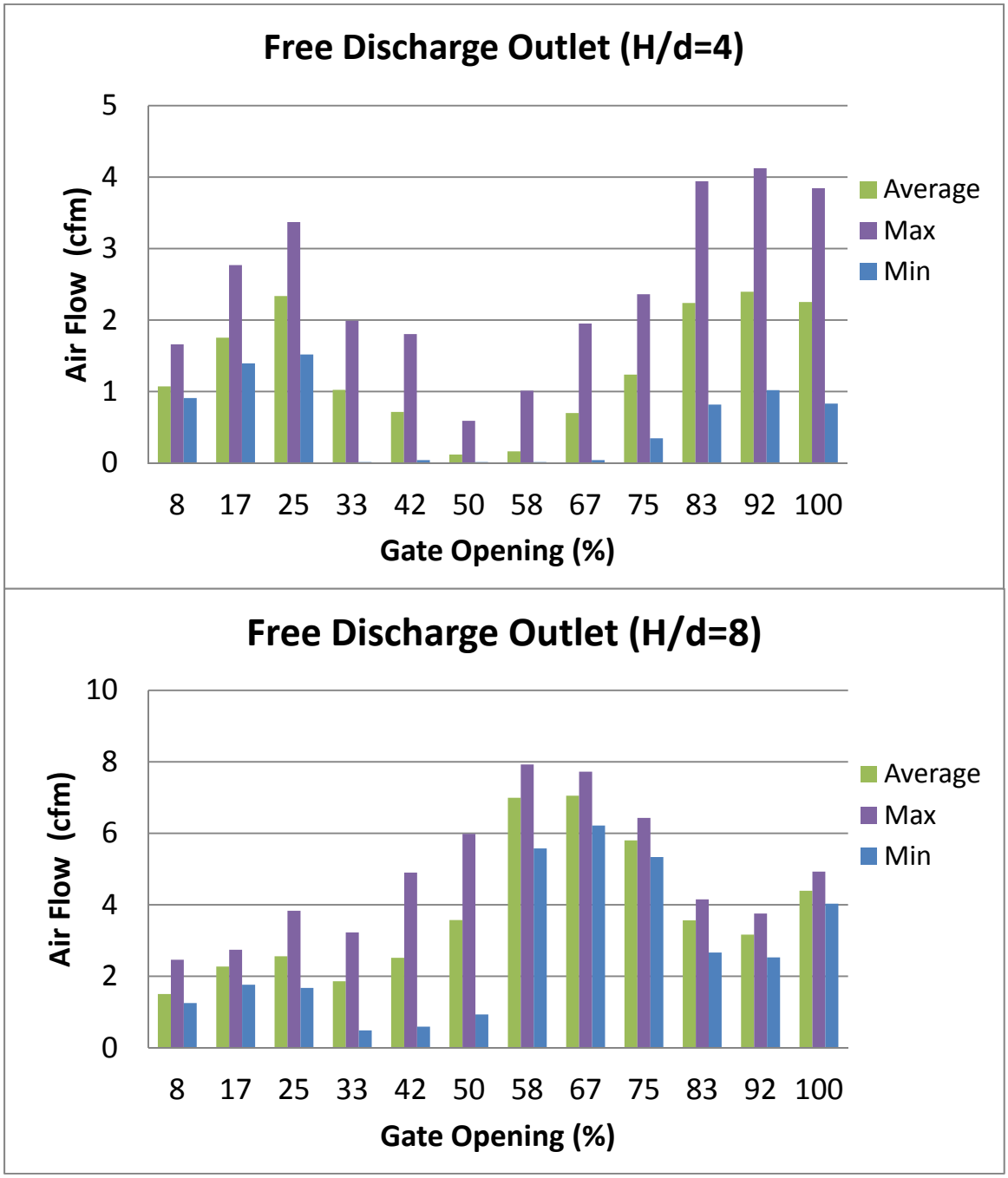
Free Discharge Outlet (H/d=4)
Air Flow (cfm)
0
1
2
3
4
5
8 17 25 33 42 50 58 67 75 83 92 100
Gate Opening (%)
Average
Max
Min
Free Discharge Outlet (H/d=8)
Air Flow (cfm)
0
2
4
6
8
10
8 17 25 33 42 50 58 67 75 83 92 100
Gate Opening (%)
Average
Max
Min

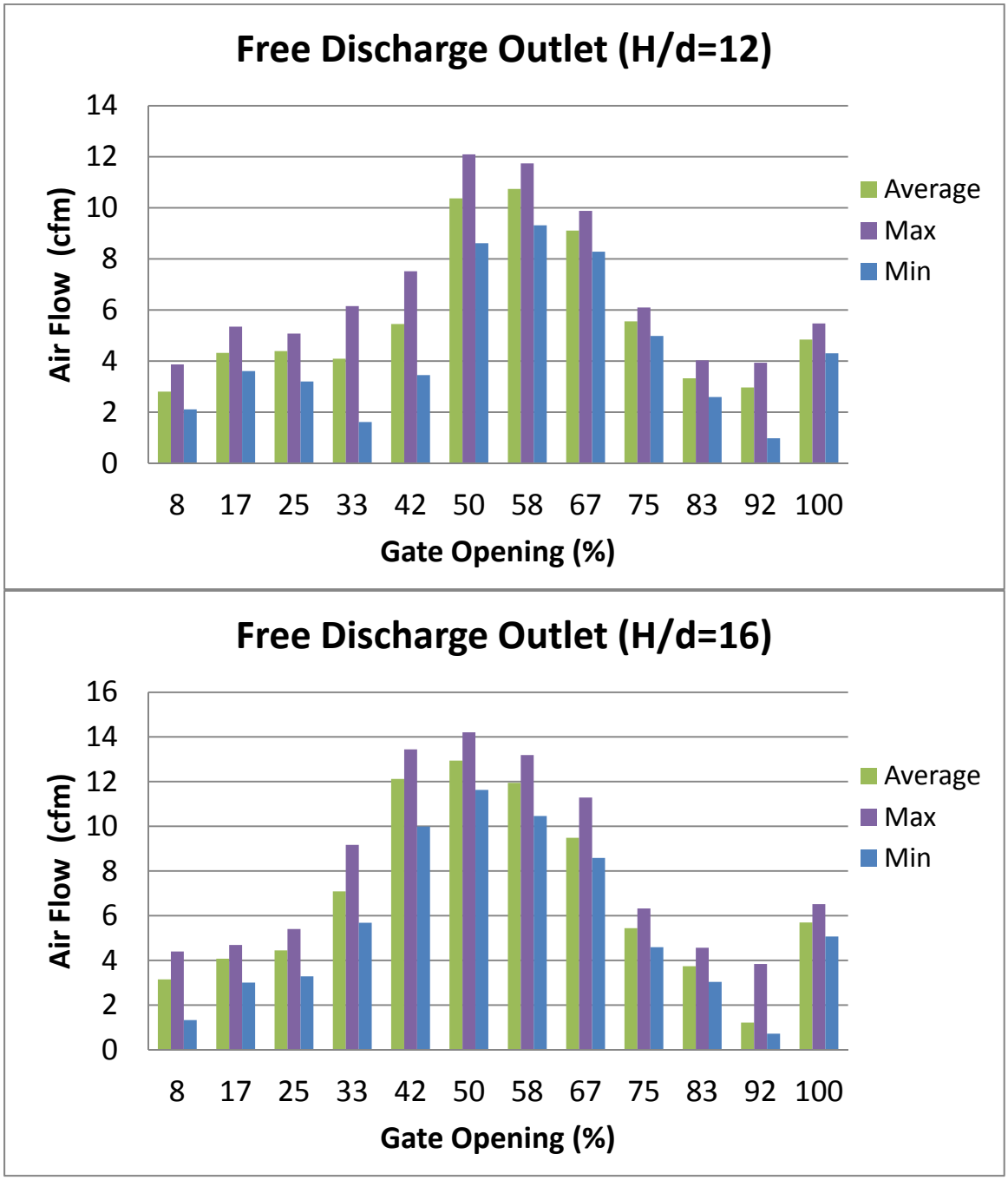
Free Discharge Outlet (H/d=12)
Air Flow (cfm)
14
12
10
8
6
4
2
0
8 17 25 33 42 50 58 67 75 83 92 100
Gate Opening (%)
Average
Max
Min
Free Discharge Outlet (H/d=16)
Air Flow (cfm)
16
14
12
10
8
6
4
2
0
8 17 25 33 42 50 58 67 75 83 92 100
Gate Opening (%)
Average
Max
Min

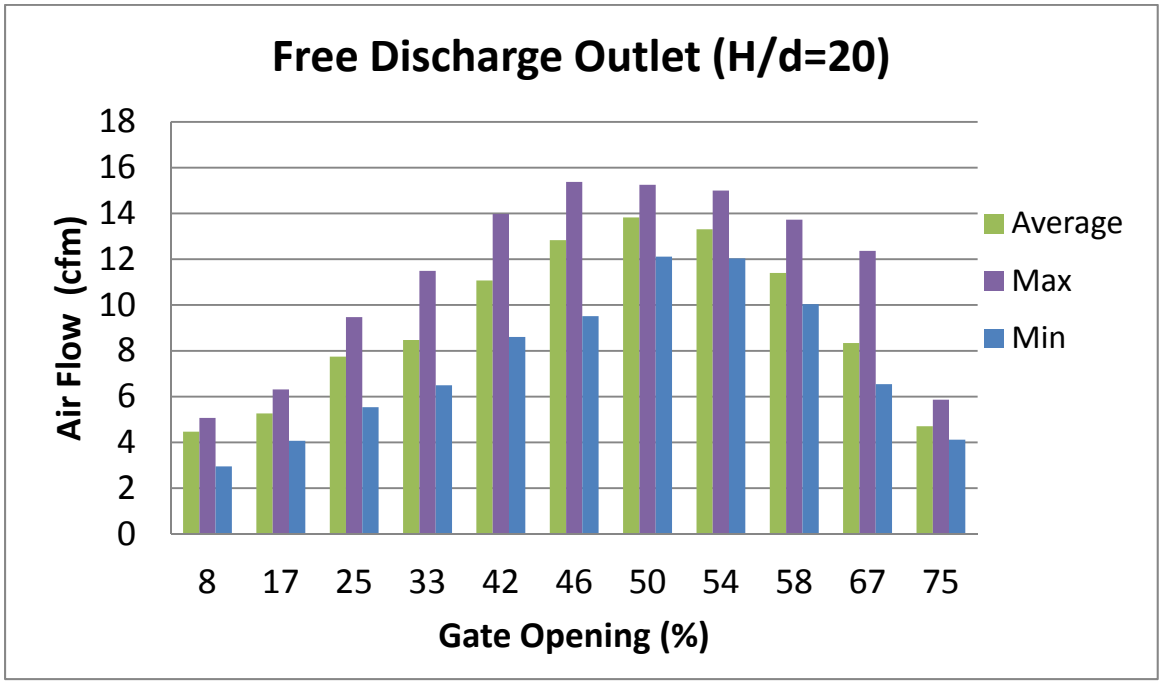
Free Discharge Outlet (H/d=20)
Air Flow (cfm)
18
16
14
12
10
8
6
4
2
0
8
17
25
33
42
46
50
54
58
67
75
Gate Opening (%)
Average
Max
Min

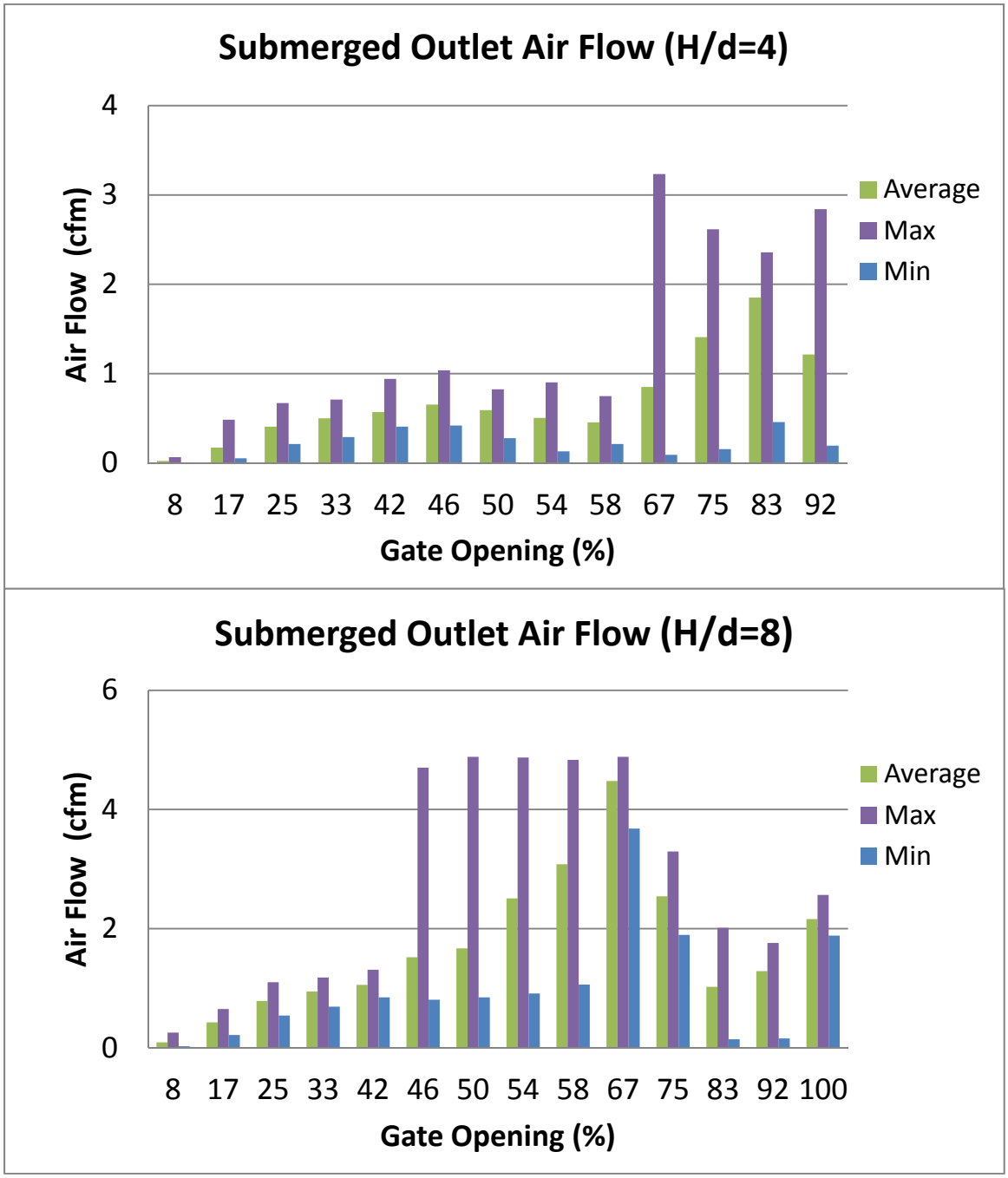
Submerged Outlet Air Flow (H/d=4)
Air Flow (cfm)
0
1
2
3
4
8 17 25 33 42 46 50 54 58 67 75 83 92
Gate Opening (%)
Average
Max
Min
Submerged Outlet Air Flow (H/d=8)
Air Flow (cfm)
0
2
4
6
8 17 25 33 42 46 50 54 58 67 75 83 92 100
Gate Opening (%)
Average
Max
Min

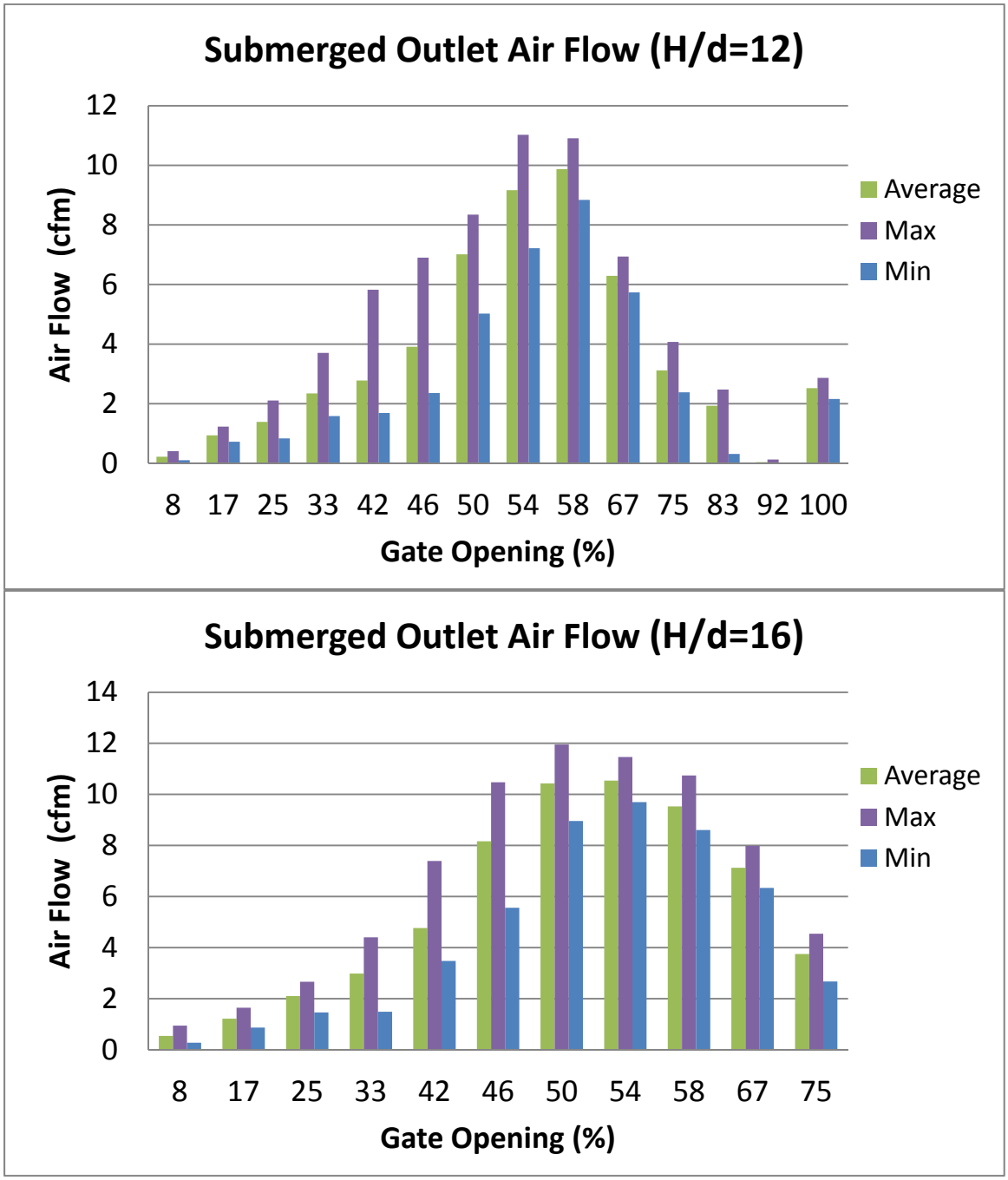
Submerged Outlet Air Flow (H/d=12)
Air Flow (cfm)
0
2
4
6
8
10
12
8 17 25 33 42 46 50 54 58 67 75 83 92 100
Gate Opening (%)
Average
Max
Min
Submerged Outlet Air Flow (H/d=16)
Air Flow (cfm)
0
2
4
6
8
10
12
14
8 17 25 33 42 46 50 54 58 67 75
Gate Opening (%)
Average
Max
Min

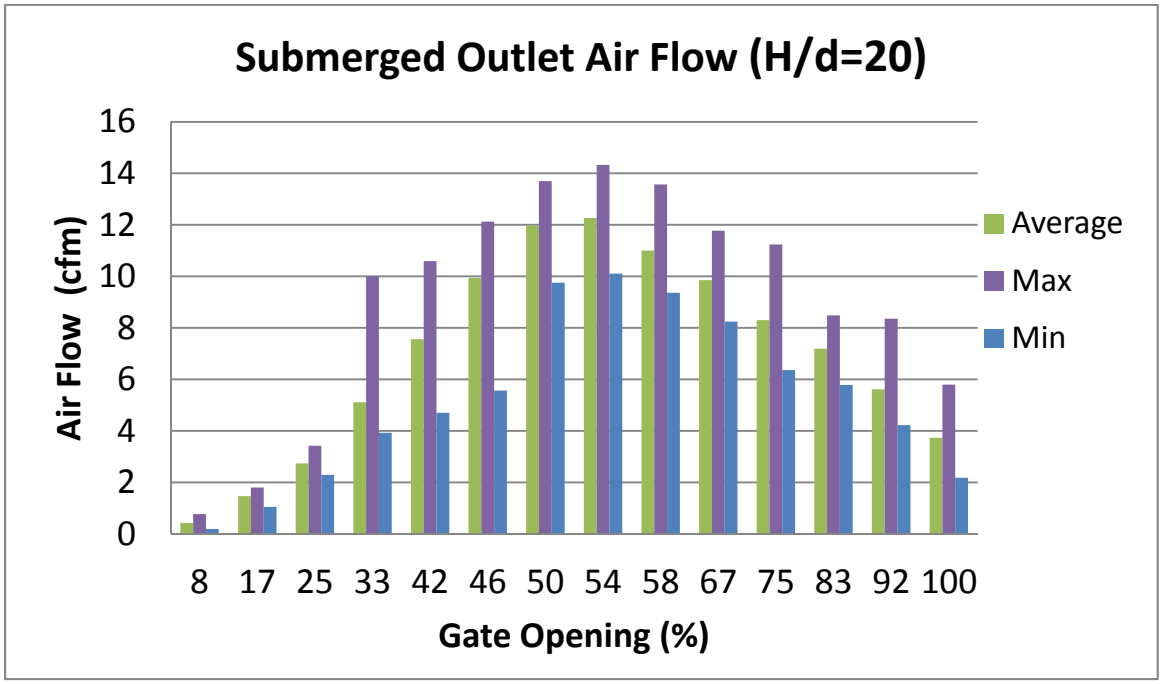
Submerged Outlet Air Flow (H/d=20)
Air Flow (cfm)
16
14
12
10
8
6
4
2
0
8 17 25 33 42 46 50 54 58 67 75 83 92 100
Gate Opening (%)
Average
Max
Min

Appendix C: Steps to Calculate C_d Values

In order to calculate the C_d values, several intermediate calculations were necessary including the friction factor, Reynolds number and a valve loss coefficient (K_L). The energy equation is used to balance the driving head and head losses (friction and minor) There representative equations are shown below:

$$f = \frac{1.325}{\left(Ln\left(\frac{e}{3.7d} + \frac{5.7}{\mathrm{Re}^{0.9}} \right) \right)^2} \tag{8}$$

where:

f	Friction factor (dimensionless)
e	Pipe roughness, ft (m)
d	Diameter of the discharge pipe, ft (m)
Re	Reynolds number (dimensionless) (Haestad, 2001).

The relative roughness (e) was assumed to be 0.00006 ft. (Tullis, 1989).

where:

$$\mathrm{Re} = \frac{Vd}{\nu} \tag{9}$$

V	Mean water velocity, fps (mps)
v	Kinematic viscosity, ft/s^2 (m/s^2) (Finnemore, 2002).

The friction factor was then used in a form of the Bernoulli equation to calculate a loss coefficient for the valve.

$$\frac{\Delta Z * 2g}{V^2} - \left(K_{exit} + \frac{fL}{D} \right) = K_{valve} \tag{10}$$

where:

ΔZ	Total differential in head, ft (m)
g	Acceleration due to gravity, ft/s^2 (m/s^2)
V	Mean water velocity, fps (mps)
K_{exit}	Exit loss coefficient ($K_{exit} = 1$)

The valve loss coefficient was then converted to a discharge coefficient (C_d) using the following equation:

$$C_d = \left(\frac{1}{K + 1} \right)^{0.5} \text{ (Tullis, 1989)} \tag{11}$$